

2 **Synthesis, Spectral and Thermal Characterization**
3 **with Antimicrobial Activity Studies on Some Metal**
4 **Complexes Containing Schiff Base Ligand**
5
6
7

8 **Abstract**

9 Some metal complexes of Ni(II), Zn(II), Mn(II), Sn(II), Co(II) and Cd(II) ions were
10 synthesized with three different synthesized Schiff base ligands. The ligands and metal
11 complexes were isolated in solid state from the reaction medium and characterized by molar
12 conductivity measurement, magnetic susceptibility, Infrared, electronic spectral, thermal
13 analysis and some physical measurements. The overall reactions were monitored by TLC
14 analysis. Molar conductance study have shown that all the complexes were non electrolytic in
15 nature. FTIR studies suggested that Schiff bases act as deprotonated bidentate ligands and
16 metal ions are attached with the ligands through N, O/S coordinating sites during
17 complexation reaction. Magnetic susceptibility data coupled with electronic spectra revealed
18 that Zn(II), Mn(II), Sn(II), and Cd(II) complexes have tetrahedral, Ni(II) complexes has square
19 planer and Co(II) complexes has octahedral geometry. Thermal analysis (TGA and DTG) data
20 showed the possible degradation pathway of the complexes and also indicated that most of
21 the complexes were thermally stable up to 200⁰C. The Schiff bases and their metal complexes
22 have been found moderate to strong antimicrobial activity.

23 **Keywords:** Schiff Base, Thiosemicarbazide, TGA, DTG, Antimicrobial activity

24 **1 INTRODUCTION**

25 Multidentate ligands are extensively used for the preparation of metal complexes with
26 interesting properties [1-5]. Among these ligands, Schiff bases containing nitrogen and
27 phenolic oxygen donor atoms are of considerable interest due to their potential application in
28 catalysis, medicine and material science [6-9]. Transition metal complexes of these ligands
29 exhibit varying configurations, structural liability and sensitivity to molecular environments.
30 The central metal ions in these complexes act as active sites for pharmacological agent.
31 This feature is employed for modeling active sites in biological systems.

32 Thiosemicarbazones obtained by the condensation reaction of thiosemicarbazide and
33 different aldehydes or ketones are important chemicals due to their broad profile of
34 pharmacological activity. The transition metal complexes of thiosemicarbazone are also
35 played important role in antimicrobial, antitumor and anticancer activities.

36 Therefore, in view of our interest in synthesis of new Schiff base complexes, which might
37 find application as pharmacological and as luminescence probes, we have synthesized and
38 characterized new transition metal complexes of Schiff bases formed by the condensation
39 reaction of different aldehydes and amino acids. The results of our studies are presented in
40 this article.

41 **2. Experimental**

42 **2.1 Materials and Methods**

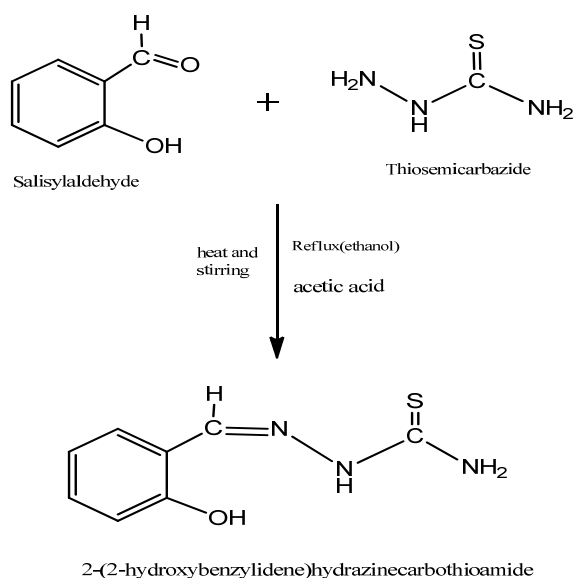
43 All chemicals and solvents used were of Analar grade. All metal(II) salts were used as
44 chloride and sulphate. The solvents such as Ethanol, methanol, chloroform, Diethyl ether,
45 petroleum ether, DMSO (dimethyl sulfoxide) and acetonitrile were purified by standard
46 procedure. The melting point or the decomposition temperature of all the prepared ligand and
47 metal complexes were observed in an electro thermal melting point apparatus model No.
48 AZ6512. Vibrational spectra (IR) were recorded with a NICOLET 310, FTIR
49 spectrophotometer, Belgium, in the range $4000-225\text{ cm}^{-1}$ with a KBr disc as reference. UV-
50 Visible spectra of the complexes in DMSO ($0.5 \times 10^{-3}\text{ M}$) were recorded in the region 200-800
51 nm on a Thermoelectron Nicolet evolution 300 UV-Visible spectrophotometer. The
52 SHERWOOD SCIENTIFIC Magnetic Susceptibility Balance that following the Gouy
53 Method were used to measure the magnetic moment of the solid complexes. The electrical
54 conductance measurements were made at room temperature in freshly prepared aqueous
55 solution (10^{-3} M) and in DMSO using a WPACM35 conductivity meter and a dip-cell with a
56 platinum electrode. some conductivity were also measured in PTI-18 Digital conductivity
57 meter. The purity of the ligand and metal complexes were tested by Thin Layer
58 Chromatography (TLC).

59

60 **2.1 Synthesis of Schiff base Ligand $\text{C}_8\text{H}_9\text{ON}_3\text{S}$ (L^1)**

61 The ligand was prepared by condensation reaction of 20 mmole of salicylaldehyde (1.048ml)
62 with 20 mmole (1.82gm) of thiosemicarbazide in a clean round bottomed flask.
63 Salicylaldehyde was dissolved in 20ml ethanol and thiosemicarbazide was dissolved in hot

64 ethanol with water. The solutions were mixed and refluxed for 3-4 hours. On cooling off
65 white colored product was formed which was washed with ethanol, acetone, and diethyl ether
66 and dried in vacuum desiccators over anhydrous CaCl_2 . The purity of ligand was tested by
67 TLC using different solvents. The product was found to be soluble in methanol, chloroform
68 and DMSO. It provided 80% yield at 34°C . The target Schiff base was synthesized according
69 to Figure-1.

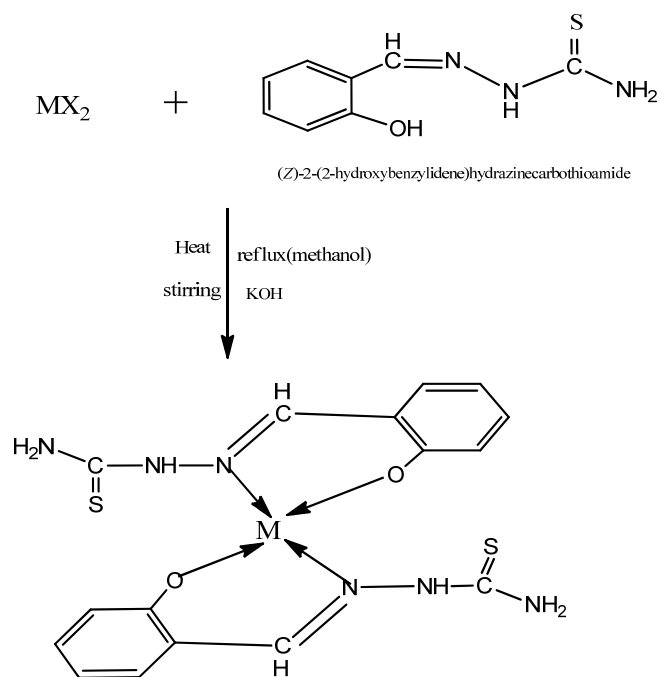


70

71 Figure-1: Synthetic pathway of Schiff base ligand $\text{C}_{14}\text{H}_{11}\text{O}_3\text{N}$ (L^1)

72 2.3 Synthesis of Metal Complexes Using Schiff Base Ligand $\text{C}_{14}\text{H}_{11}\text{O}_3\text{N}$ (L^1)

73 The synthesized complexes have the general formula $[\text{M}(\text{SB})_2]$; where $\text{M} = \text{Zn}(\text{II}), \text{Ni}(\text{II})$ and
74 $\text{Mn}(\text{II})$ and $\text{SB} =$ synthesized Schiff base ligand (Fig-3). During complexation reaction, 15ml
75 methanolic solution of Zinc(II) sulphate (0.2875g, 1mmol)/ Ni(II) chloride hexahydrate
76 (0.238g, 1mmol)/ Manganese(II) chloride tetrahydrate (0.198g, 1mmol) was taken in a two
77 necked round bottom flask and kept on a magnetic stirring. A methanolic solution (20 mL) of
78 prepared Schiff base ligand (0.390g, 2mmol) was added drop wise and a methanolic solution
79 (10mL) of KOH (0.1122g, 1mmol) was added slowly then the resultant mixture was heated
80 with constant stirring on a magnetic stirrer for 4-5 hours. On cooling colored solid product
81 was formed which was washed with methanol, acetone, ether and dried in vacuum over
82 anhydrous CaCl_2 . The reaction was monitored by TLC using petroleum ether, toluene, ethyl
83 acetate and methanol as solvent. The common structure of metal complexes has been shown
84 in (Figure-2-6).

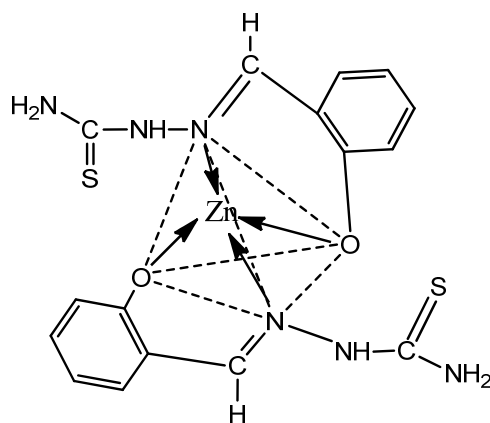


85

86 Figure-2: Synthetic pathway of Schiff Base Ligand (L^2) Metal Complexes

87 Where, $M=Zn(II)$, $Ni(II)$, $Mn(II)$, and $Sn(II)$ ions and $X=Cl^-$, SO_4^{2-} ions

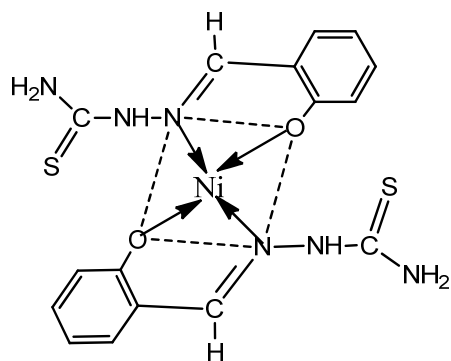
88



89

90 Figure-3: Structure of $[C_{16}H_{16}ZnO_2N_6S_2]$ Comp

91

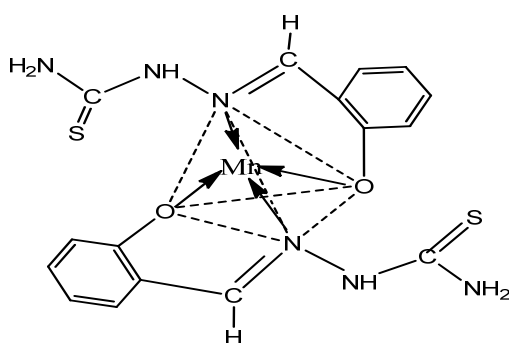


92

93

Figure-4: Structure of $[C_{16}H_{16}NiO_2N_6S_2]$ Complex

94

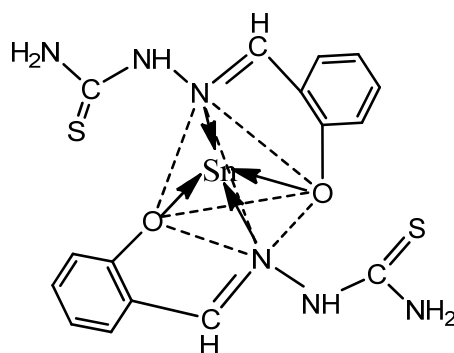


95

96

Figure-5: Structure of $[C_{16}H_{16}MnO_2N_6S_2]$ Complex

97



98

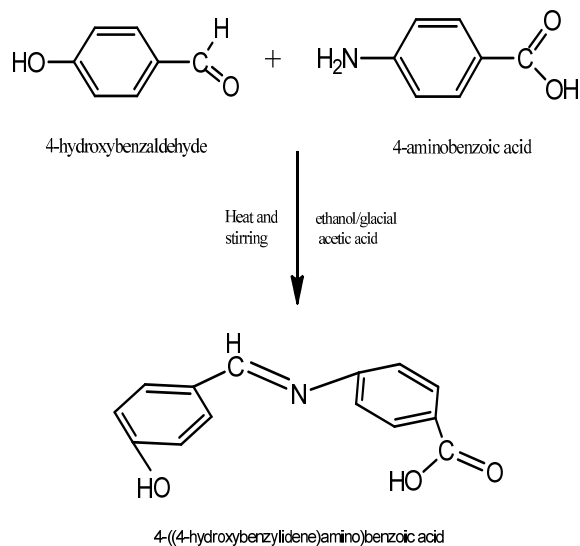
99

Figure-6: Structure of $[C_{16}H_{16}SnO_2N_6S_2]$ Complex

100 2.4 Synthesis of Schiff Base Ligand $C_{14}H_{11}O_3N$ (L^2)

101 4-hydroxy benzaldehyde (2.44g, 20 mmol) dissolved in absolute ethanol (20-25 mL) was
 102 added **dropwise** to a constant stirring solution of 4-aminobenzoic acid(2.76 g, 20 mmol) in 30
 103 mL ethanol and 2 mL of conc. glacial acetic acid was added slowly. Then the mixture was
 104 refluxed for (4-5)h. On cooling, a solid yellow product was formed which was filtered,

105 washed with ethanol and diethyl ether and dried in vacuum over anhydrous CaCl_2 . The
106 reaction was monitored by TLC using petroleum ether, ethyl acetate, toluene and methanol
107 solvents. The product was found to be soluble in methanol, chloroform and DMSO. It
108 provided 65% yield at 34°C . The target Schiff base was synthesized according to Figure-7.



109

110

Figure-7: Synthetic pathway of Schiff base ligand $\text{C}_{14}\text{H}_{11}\text{O}_3\text{N}$ (L^2)

111

2.5 Synthesis of Metal Complex Using Schiff Base Ligand (L^2)

112

113

114

115

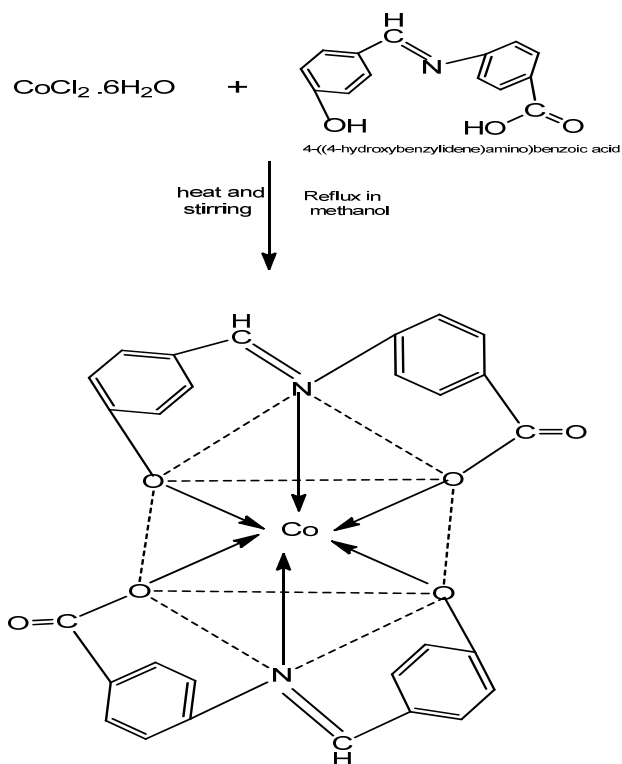
116

117

118

119

The complex was prepared in 1:2 molar ratio (metal : ligand). A methanolic solution (20 mL) of cobalt(II) chloride hexahydrate (0.24 g, 1 mmol) was taken in a two necked round bottom flask and kept on magnetic stirring and a methanolic solution (20 mL) of prepared Schiff base ligand (0.483 g, 2 mol) was added dropwise and stirred with heating for 4-5h. On cooling, precipitate was formed which was filtered, washed with ethanol, acetone, and diethyl ether and dried in vacuum desiccators over anhydrous CaCl_2 . The purity of complex was tested by TLC using different solvents. The complex was soluble in DMSO with heat. The proposed structure of complex was shown in (Figure-8).

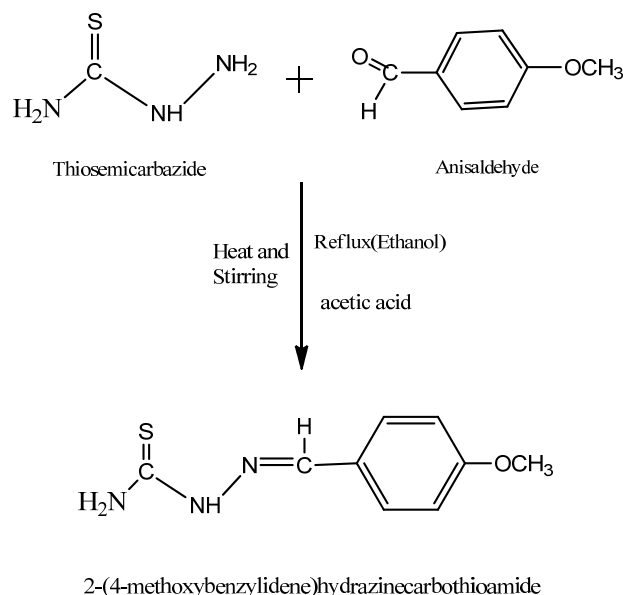


120

121 Figure-8: Synthetic pathway of Co(II) complex with Schiff Base Ligand (L^2)

122 **2.6 Synthesis of Schiff base Ligand $C_9H_{11}N_3OS$ (L^3)**

123 To a stirring solution of thiosemicarbazide (0.91 gm, 10 mmol) dissolved in 20mL of ethanol
 124 with water, a solution of Anisaldehyde(1.22mL,10mmol) in 10mL ethanol was added dropwise.
 125 After sometime 2ml of glacial acetic acid was added with the reaction mixture and the solution
 126 was refluxed for 5-6 h and allowed to cool overnight in room temperature. The off white
 127 product was filtered washed several times with ethanol and finally with diethyl ether and dried in
 128 vacuum over anhydrous CaCl_2 . The reaction was monitored by TLC using petroleum ether,
 129 ethyl acetate, toluene and methanol solvents .The product was found to be soluble in methanol,
 130 DMF and DMSO. It provided 62% yield. The Schiff base was synthesized according to
 131 Figure-9.



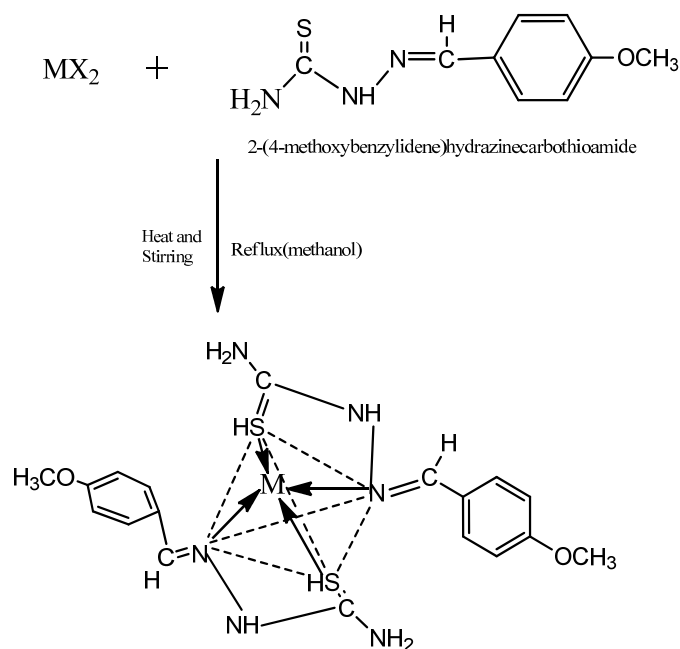
132

133

Figure-9: Synthetic pathway of Schiff base ligand $C_9H_{11}N_3OS$ (L^3)

134 **2.7 Synthesis of Metal Complex Using Schiff Base Ligand (L^3):**

135 The complex was prepared in 1:2 molar ratio (metal : ligand). Methanolic solution (20 mL) of
 136 cadmium(II) chloride dihydrate (0.228g, 1mmol) was taken in a two necked round bottom
 137 flask and kept on magnetic stirring. A methanolic solution (20 mL) of prepared Schiff base
 138 ligand (L^3) (0.418g, 2mmol) was added dropwise and stirred with heating for 4-5h. On
 139 cooling, precipitate was formed which was filtered, washed with ethanol, acetone, and diethyl
 140 ether and dried in vacuum desiccators over anhydrous $CaCl_2$. The reaction was monitored by
 141 TLC using different solvents. The complex was soluble in DMSO with heat. The proposed
 142 structure of complex was shown in (Figure-10).



143

144

Figure-10: Synthetic pathway of Schiff Base Ligand (L^4) Metal Complex

145

Where, $M=\text{Cd(II)}$ ions

146

3. Characterization of the Ligands and Complexes

147

The structures of the complexes were characterized by melting point, conductivity measurements, magnetic susceptibility, IR spectra and UV visible spectra [10] analysis. The purity of the ligands and metal complexes was monitored by Thin Layer Chromatography

149

150

151

152

3.1 Melting point

153

Melting point gives an approximate idea about the nature of the complexes and can suggest whether it is covalent or ionic [11]. The melting point of all the synthesized ligands and complexes are shown in Table-1.

154

155

156

157

Table-1: Physical characteristics and analytical data of ligands and complexes

| Compound/Empirical Formula | Formula Weight | Color | Yield(%) | Melting Point/ Decomposition temp.($^{\circ}\text{C}$) |
|----------------------------|----------------|-------|----------|--|
| | | | | |

| | | | | |
|--|--------|-----------------|------|---|
| Ligand (L ¹) C ₈ H ₉ ON ₃ S | 195 | off white | 80 % | 215 ⁰ C - 217 ⁰ C |
| [Zn (L ¹) ₂] .2H ₂ O [ZnC ₁₆ H ₁₆ O ₂ N ₆ S ₂].2H ₂ O | 491.38 | cream color | 67 % | above 300 ⁰ C |
| [Ni (L ¹) ₂].H ₂ O [NiC ₁₆ H ₁₆ O ₂ N ₆ S ₂].H ₂ O | 466.93 | yellow green | 70 % | 275 ⁰ C - 280 ⁰ C |
| [Mn (L ¹) ₂] .H ₂ O [MnC ₁₆ H ₁₆ O ₂ N ₆ S ₂].H ₂ O | 462.94 | golden rod | 65 % | 275 ⁰ C - 280 ⁰ C |
| [Sn (L ¹) ₂] [SnC ₁₆ H ₁₆ O ₂ N ₆ S ₂] | 508.71 | greenish yellow | 60% | 240 ⁰ C - 250 ⁰ C |
| Ligand (L ²) C ₁₄ H ₁₁ O ₃ N | 241 | yellow | 65 % | 241 ⁰ C - 245 ⁰ C |
| [Co(L ²) ₂] .2H ₂ O [CoC ₂₈ H ₁₈ O ₆ N ₂].2H ₂ O | 576.93 | golden rod | 56 % | above 300 ⁰ C |
| Ligand (L ³) C ₉ H ₁₁ N ₃ OS | 209 | off white | 62% | 145 ⁰ C - 150 ⁰ C |
| [Cd(L ³) ₂] [CdC ₁₈ H ₂₂ O ₂ N ₆ S ₂] | 530.41 | white | 75 % | 260 ⁰ C - 265 ⁰ C |

158

159 3.2 Characterizations by Conductivity

160

161 The molar conductivities were obtained using the formula

$$162 \quad \Lambda = \frac{1000}{C} \times \text{Cell constant} \times \text{Observed conductivity.}$$

163 Where, Λ =molar conductance

164 C= concentration

165 The molar conductance is calculated from the measured specific conductance at room
166 temperature by using the above equation. The experimental results are shown in Table-2.

167

168

169 **Table-2:** Data for the determination of Molar conductivity

| Name of Complex | Observed conductivity (ohm ⁻¹ cm ² mol ⁻¹) | Molar conductance Λ $= (1000/c)$ $\times \text{specific conductance}$ $S\text{cm}^2\text{mol}^{-1}$ | μ_{eff} in B.M. | No. of unpaired electron |
|--|---|---|----------------------------|--------------------------|
| [Zn(L ¹) ₂].2H ₂ O [ZnC ₁₆ H ₁₆ O ₂ N ₆ S ₂].2H ₂ O | 3 | 3 | 0.567 | – |
| [Ni(L ¹) ₂].H ₂ O [NiC ₁₆ H ₁₆ O ₂ N ₆ S ₂].H ₂ O | 6 | 6 | 1.471 | – |
| [Mn(L ¹) ₂].H ₂ O [MnC ₁₆ H ₁₆ O ₂ N ₆ S ₂].H ₂ O | 8 | 8 | 2.576 | 1 |
| [Sn(L ¹) ₂] [SnC ₁₆ H ₁₆ O ₂ N ₆ S ₂] | 9 | 9 | 0.639 | – |
| [Co(L ²) ₂].2H ₂ O [CoC ₂₈ H ₁₈ O ₆ N ₂].2H ₂ O | 8 | 8 | 4.017 | 3 |
| [Cd(L ³) ₂] [CdC ₁₈ H ₂₂ O ₂ N ₆ S ₂] | 6 | 6 | 0.461 | – |

170

171 From the above table data it is showed that all the complexes are non-electrolyte.

172 **3.3 Characterizations by Magnetic Susceptibility**

173 **Measurement of magnetic susceptibility:** The measurements of magnetic susceptibilities
174 were made at about constant temperature; Curie-law was used and was calculated from the
175 equation.

$$176 \quad \mu_{\text{eff}} = 2.83 \sqrt{\chi_m^{\text{corr}} \cdot T} \quad \text{B.M.}$$

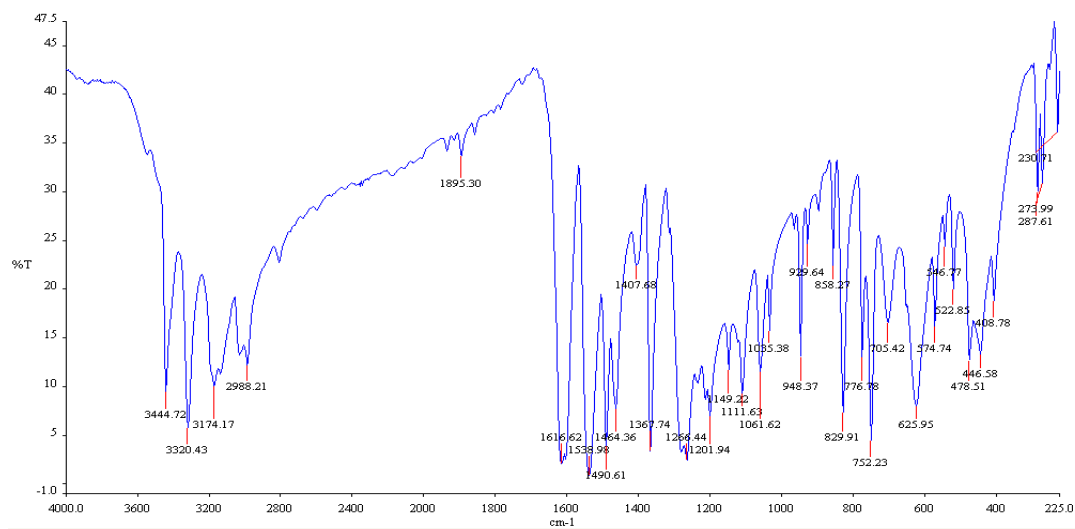
177 Thus μ_{eff} obtained is known as effective magnetic moment. All the values and weight were
178 expressed in C.G.S. units. The observed values of effective magnetic moment (μ_{eff}) of the
179 complexes at room temperature are given in table 2. From the above data it is showed that the
180 Zn(II), Ni(II), Sn(II) and Cd(II) ions complexes are diamagnetic and Mn(II) and Co(II) ions
181 complexes are paramagnetic in nature[13].

182 **3.4 Measurement of IR spectra:** At first the complexes heat six hour and KBr overnight in oven.
183 Then the complexes and KBr grind with pestle in mortar. Infrared spectra disc were recorded as
184 KBr with a NICOLET 310, FTIR spectrophotometer, Belgium, from 4000-225 cm^{-1} .

185 3.4.1 IR spectra of Schiff Base ligand $\text{C}_8\text{H}_9\text{ON}_3\text{S}$ (L^1) and It's metal complexes

186 a. IR spectra of Schiff Base ligand $\text{C}_8\text{H}_9\text{ON}_3\text{S}$ (L^1)

187 The spectrum of ligand showed a strong absorption band at 1616 cm^{-1} due to the azomethine
188 $\nu(\text{C}=\text{N})$ stretching frequency of the free ligand [14-18] indicating that the condensation have
189 taken place between the CHO moiety of salisylaldehyde and $-\text{NH}_2$ moiety of
190 thiosemicarbazide. The IR spectra of the free ligand (figure-11) showed two bands at 3320
191 cm^{-1} and 3174 cm^{-1} may be attributed to the free $-\text{NH}_2$ and $\nu(\text{N}-\text{H})$ groups respectively.
192 These bands remains in the same region in all complexes spectra, suggesting nonparticipation
193 in coordination of one terminal $-\text{NH}_2$ group in thiosemicarbazone [15,19-21] The band
194 observed at 3444 cm^{-1} was assigned to the $\nu(\text{O}-\text{H})$ of hydroxyl group [14,15,22]. The strong
195 band 776 cm^{-1} for $\nu(\text{C}=\text{S})$ indicated that $\text{C}=\text{S}$ bond was present in the Schiff base ligand
196 [14,22].

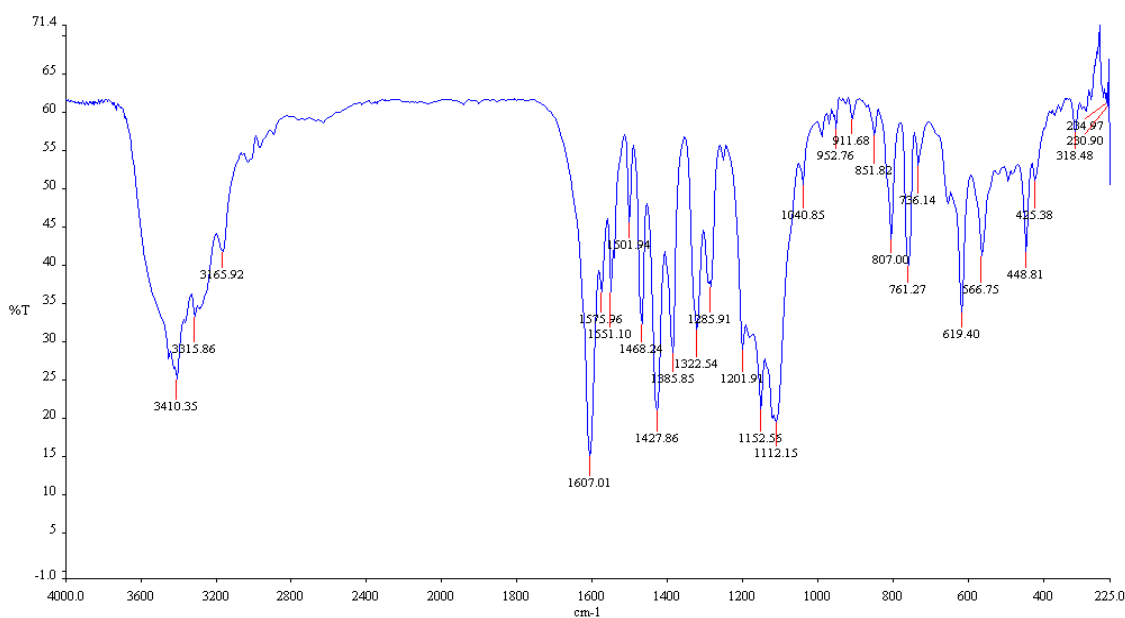


197
198 Figure-11: IR spectra of Schiff base ligand $\text{C}_8\text{H}_9\text{ON}_3\text{S}$ (L^1)

199 b. IR spectra of $[\text{ZnC}_{16}\text{H}_{16}\text{O}_2\text{N}_6\text{S}_2] \cdot 2\text{H}_2\text{O}$ complex

200 In order to determine the mode of coordination of ligand to metal in complexes, IR spectrum
201 of ligand was compared with IR spectrum of metal complexes (figure-12). The band at 1616
202 cm^{-1} due to the azomethine $\nu(\text{C}=\text{N})$ stretching frequency of the free ligand that shifted to
203 lower frequency in the spectra of the Zn (II) complex at 1607 cm^{-1} which indicated the

204 coordination through azomethine N atom. The band 3444 cm^{-1} due to the $\nu(\text{O-H})$ of hydroxyl
 205 group in the IR spectra of the ligand was absent and shifted to lower absorption frequency in
 206 the IR spectra of Ni(II) complex indicated the coordination through the phenolic oxygen
 207 [23,24]. This is confirmed by the shift of $\nu(\text{C-O})$ stretching vibration observed at 1266 cm^{-1}
 208 in the spectra of free ligand to 1285 cm^{-1} stretching vibration of complex after coordination
 209 [16], which corresponds to forming of weaker C-O(Zn) bond comparing to C-O(H) and
 210 confirms coordination of ligand to Ni(II) via deprotonated phenolic oxygen [25,26]. Also the
 211 medium intensity bands observed at 566 cm^{-1} is attributed to M-O and 448 cm^{-1} is attributed to
 212 M-N bonds [27].



213

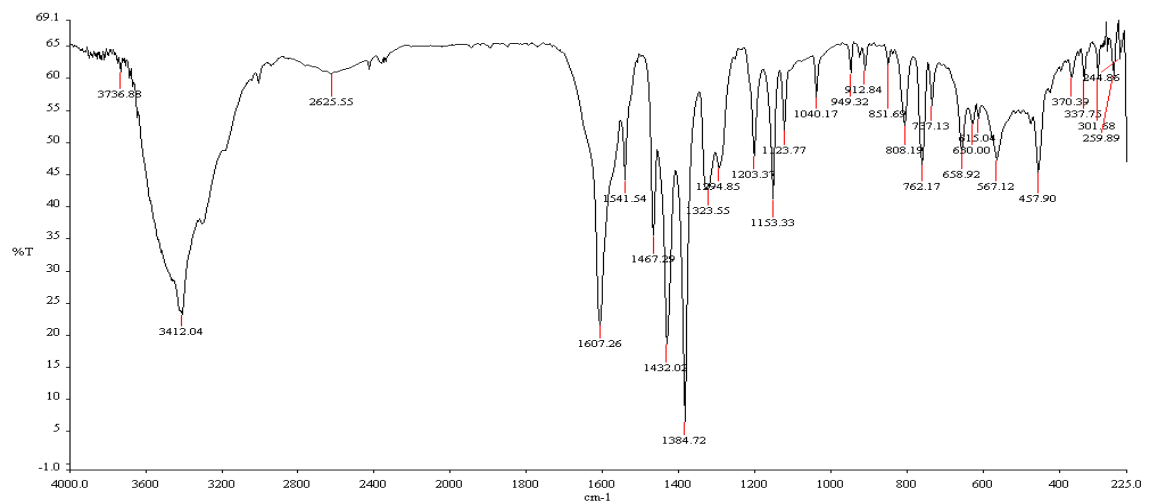
Figure-12: IR spectra of $[\text{ZnC}_{16}\text{H}_{16}\text{O}_2\text{N}_6\text{S}_2]\cdot 2\text{H}_2\text{O}$ complex

214

215 **c. IR spectra of $[\text{NiC}_{16}\text{H}_{16}\text{O}_2\text{N}_6\text{S}_2]\cdot \text{H}_2\text{O}$ complex**

216 In order to determine the mode of coordination of ligand to metal in complexes IR spectrum
 217 of ligand was compared with IR spectrum of metal complexes [14, 23]. The band at 1616 cm^{-1}
 218 ¹ due to the azomethine $\nu(\text{C=N})$ stretching frequency of the free ligand that shifted to lower
 219 frequency in the spectra of the Ni(II) complex (figure-13) at 1607 cm^{-1} indicating the
 220 coordination through N atom [5-9]. The band 3444 cm^{-1} due to the $\nu(\text{O-H})$ of hydroxyl
 221 group in the IR spectra of the ligand was absent and shifted to lower absorption frequency in
 222 the IR spectra of Ni(II) complex indicated the coordination through the phenolic oxygen
 223 [22,24]. This is confirmed by the shift of $\nu(\text{C-O})$ stretching vibration observed at 1266 cm^{-1}
 224 in the spectra of free ligand to 1294 cm^{-1} stretching vibration of complex after coordination

225 [16], which corresponds to forming of weaker C-O(Ni) bond comparing to C-O(H) and
226 confirms coordination of ligand to Ni(II) via deprotonated phenolic oxygen. Also the medium
227 intensity bands observed at 567 cm^{-1} is attributed to M-O and 457 cm^{-1} is attributed to M-N
228 bonds [27].



229

230 Figure-13: IR spectra of $[\text{NiC}_{16}\text{H}_{16}\text{O}_2\text{N}_6\text{S}_2]\cdot\text{H}_2\text{O}$

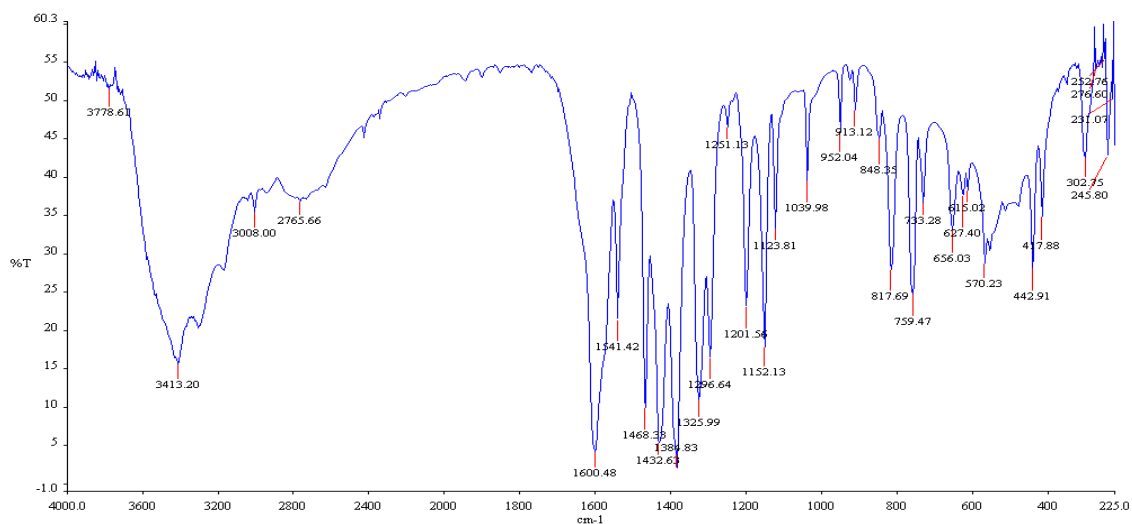
230

231 d. IR spectra of $[\text{MnC}_{16}\text{H}_{16}\text{O}_2\text{N}_6\text{S}_2]$

232 In order to determine the mode of coordination of ligand to metal in complexes IR spectrum
233 of ligand was compared with IR spectrum of metal complexes. The band at 1616 cm^{-1} due to
234 the azomethine $\nu(\text{C}=\text{N})$ stretching frequency of the free ligand that shifted to lower frequency
235 in the spectra of the Mn(II) complex (figure-14) at 1600 cm^{-1} indicating the coordination
236 through N atom. The band 3444 cm^{-1} due to the $\nu(\text{O}-\text{H})$ of hydroxyl group in the IR spectra
237 of the ligand was absent and shifted to lower absorption frequency in the IR spectra of Mn(II)
238 complex indicated the coordination through the phenolic oxygen. This is confirmed by the
239 shift of $\nu(\text{C}-\text{O})$ stretching vibration observed at 1266 cm^{-1} in the spectra of free ligand to
240 1296 cm^{-1} stretching vibration of complex after coordination, which corresponds to forming
241 of weaker C-O(Mn) bond comparing to C-O(H) and confirms coordination of ligand to
242 Mn(II) via deprotonated phenolic oxygen [5,17]. Also the medium intensity bands observed
243 at 570 cm^{-1} is attributed to M-O and 442 cm^{-1} is attributed to M-N bonds [27].

244

245



246

247

Figure-14: IR spectra of [MnC₁₆H₁₆O₂N₆S₂].H₂O

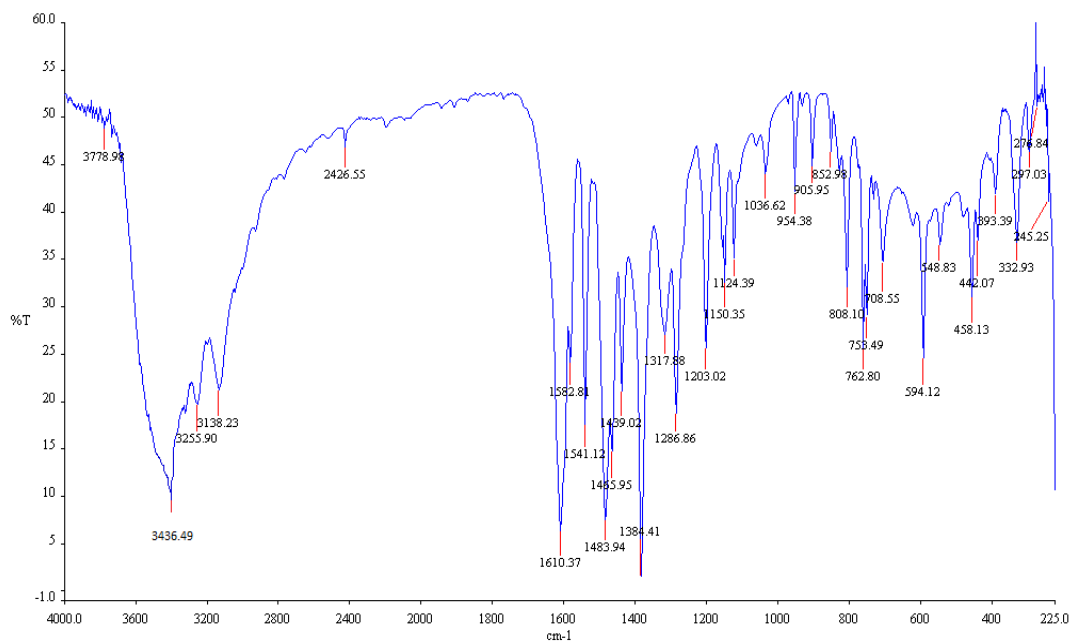
248

e. IR spectra of [SnC₁₆H₁₆O₂N₆S₂]

249

In order to determine the mode of coordination of ligand to metal in complexes IR spectrum of ligand was compared with IR spectrum of metal complexes. The band at 1616 cm⁻¹ due to the azomethine $\nu(\text{C}=\text{N})$ stretching frequency of the free ligand that shifted to lower frequency in the spectra of the Sn(II) complex (figure-15) at 1610 cm⁻¹ indicating the coordination through N atom. The band 3444 cm⁻¹ due to the $\nu(\text{O}-\text{H})$ of hydroxyl group in the IR spectra of the ligand was absent and shifted to lower absorption frequency in the IR spectra of Sn(II) complex indicated the coordination through the phenolic oxygen. This is confirmed by the shift of $\nu(\text{C}-\text{O})$ stretching vibration observed at 1266 cm⁻¹ in the spectra of free ligand to 1286 cm⁻¹ stretching vibration of complex after coordination, which corresponds to forming of weaker C-O(Sn) bond comparing to C-O(H) and confirms coordination of ligand to Sn(II) via deprotonated phenolic oxygen. Also the medium intensity bands observed at 594cm⁻¹ is attributed to M-O and 458cm⁻¹ is attributed to M-N bonds.

262



263

264

Figure-15: IR spectra of [SnC₁₆H₁₆O₂N₆S₂]

265

Table-3: FTIR spectral data of the ligand C₈H₉ON₃S (L¹) and it's metal complexes (in cm⁻¹)

| Ligand / Metal Complexes | IR/cm ⁻¹ | | | | |
|---|---------------------|--------|--------|--------|--------|
| | ν(O-H) | ν(C=N) | ν(C-O) | ν(M-O) | ν(M-N) |
| C ₈ H ₉ ON ₃ S | 3444 | 1616 | 1266 | - | - |
| [ZnC ₁₆ H ₁₆ O ₂ N ₆ S ₂].2H ₂ O | 3410 | 1607 | 1285 | 566 | 448 |
| [NiC ₁₆ H ₁₆ O ₂ N ₆ S ₂].H ₂ O | 3412 | 1607 | 1294 | 567 | 457 |
| [MnC ₁₆ H ₁₆ O ₂ N ₆ S ₂].H ₂ O | 3413 | 1600 | 1296 | 570 | 442 |
| [SnC ₁₆ H ₁₆ O ₂ N ₆ S ₂] | 3436 | 1610 | 1286 | 594 | 458 |

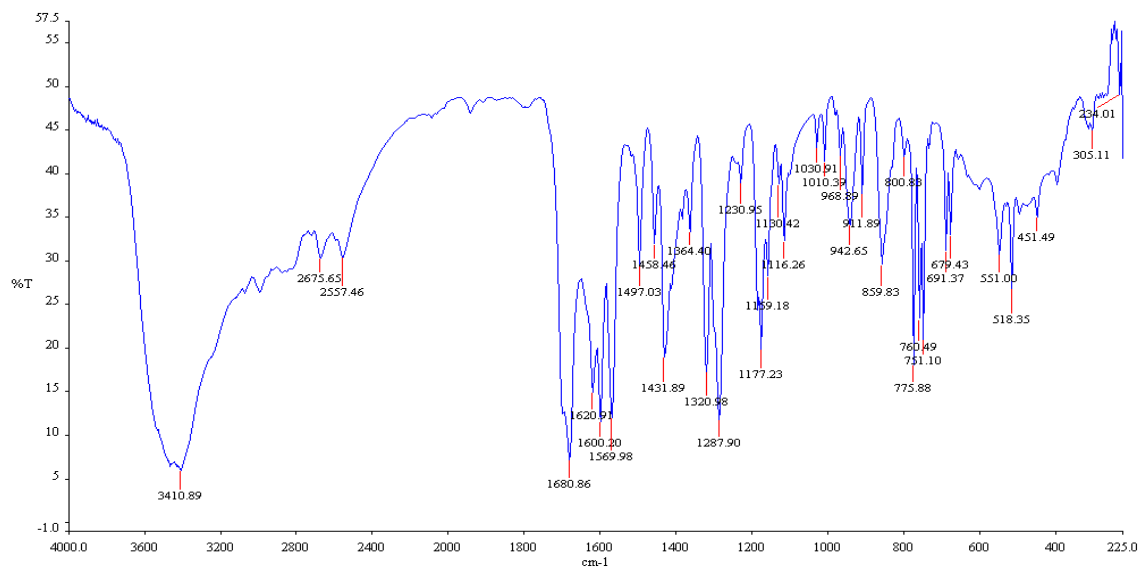
266

267 3.4.2 IR spectra of Schiff Base ligand C₁₄H₁₁O₃N (L²) and It's metal complex

268 a. IR spectra of Schiff Base ligand C₁₄H₁₁O₃N (L²)

269 The bands at 1735 cm⁻¹ and 3420 cm⁻¹ due to carbonyl (C=O) and NH₂ stretching vibrations
 270 of the starting reagents respectively were absent in the spectra of ligand (figure-16) and a
 271 strong new band at 1620 cm⁻¹ was appeared which assigned to the azomethine (HC=N)
 272 linkage, a fundamental feature of Schiff base ligand [28,29]. This indicated that amino and

273 aldehyde moieties of the starting reagents have been converted into the azomethine moiety.
274 The bands at 1320 cm^{-1} due to $\nu(\text{C-O})$ of phenolic group and 3410 cm^{-1} due to the phenolic
275 $\nu(\text{OH})$ were also observed in the spectra of ligand [23]. The bands at 1680 cm^{-1} due to
276 $\nu(\text{C=O})$ stretching vibration and 3080 cm^{-1} due to carboxylic $-\nu(\text{OH})$ were observed in the
277 IR spectra of ligand [30-33].



278

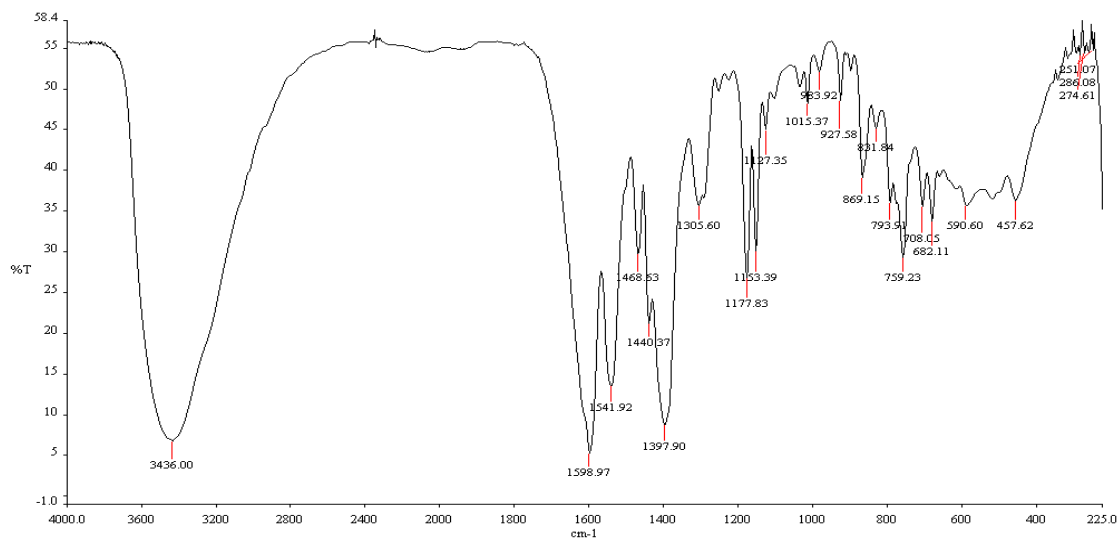
279 Figure-16: IR Spectra of 4-((hydroxybenzylidene)amino)benzoic acid ligand(L^2)

280

281 b. IR Spectra of $[\text{CoC}_{28}\text{H}_{18}\text{O}_6\text{N}_2]\cdot 2\text{H}_2\text{O}$

282 The band at 1620 cm^{-1} due to the azomethine $-\text{HC}=\text{N}$ stretching vibration was shifted to
283 lower frequency at 1541 cm^{-1} in the metal complex compared to free ligand, suggested the
284 coordination of metal ion through nitrogen of azomethine group [34-36]. The N atom of
285 azomethine would reduce the electron density in the azomethine link and thus lower the
286 $\text{HC}=\text{N}$ absorption after coordination. This is further substantiate by the presence of a new
287 band at 457 cm^{-1} assignable to $\nu(\text{M-N})$. The disappearance of phenolic $\nu(\text{OH})$ band at 3410
288 cm^{-1} in Co(II) complex suggested the co-ordination by the phenolic oxygen after
289 deprotonation to the metal ions. This is further supported by shifting of $\nu(\text{C-O})$ phenolic
290 band at 1320 cm^{-1} to lower wave number at 1305 cm^{-1} in the metal complex. The appearance
291 of a new band at 590 cm^{-1} due to $\nu(\text{M-O})$ in the Co(II) complex (figure-17) which further
292 substantiate . The band at 1680 cm^{-1} assigned to $\nu(\text{C=O})$ in the spectra of ligand also shifted
293 to lower frequency range in the metal complex. That suggested the involvement of oxygen
294 atom of carboxylic $\nu(-\text{OH})$ group to the coordination with metal ions. The comparison of the

295 IR spectra of the Schiff base and its metal chelates indicated that the Schiff base ligand
 296 coordinated to metal ions by three donor atoms representing the ligand acting in a tri-
 297 dentative manner.



298

Figure-17: IR Spectra of $[\text{CoC}_{28}\text{H}_{18}\text{O}_6\text{N}_2]\cdot 2\text{H}_2\text{O}$ with ligand (L^2)

299

300 **Table-4:** FTIR spectral data of the ligand L^2 and its Co(II) metal complex (in cm^{-1})

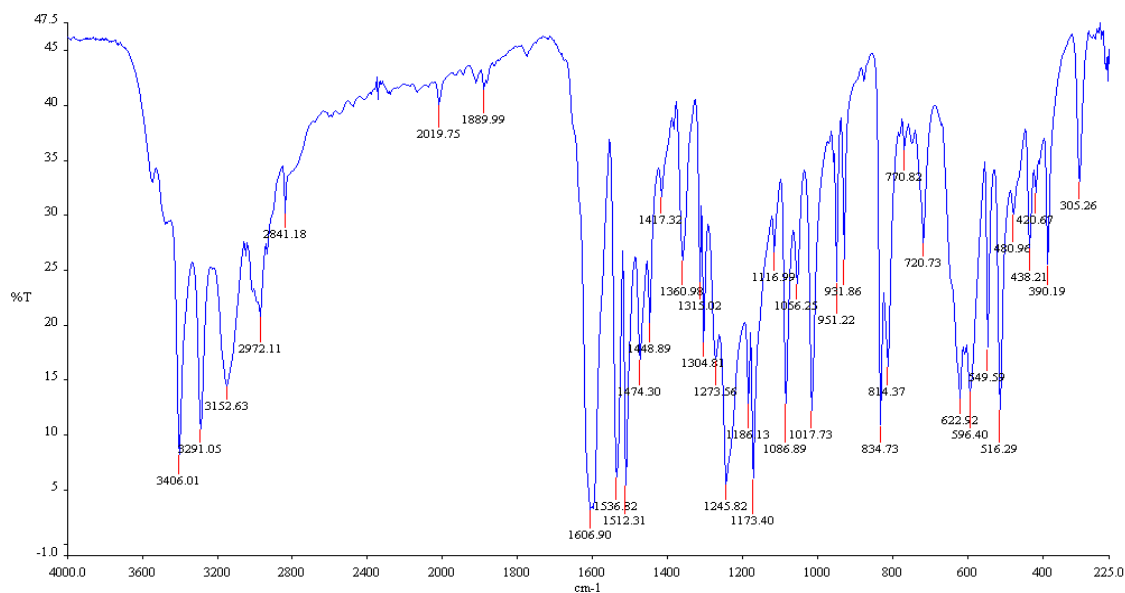
| Ligand / Metal Complexes | IR/ cm^{-1} | | | | | |
|---|----------------------|-------------------|-------------------|-------------------|-------------------|-------------------|
| | $\nu(\text{O-H})$ | $\nu(\text{C=N})$ | $\nu(\text{C=O})$ | $\nu(\text{C-O})$ | $\nu(\text{M-O})$ | $\nu(\text{M-N})$ |
| $\text{C}_{14}\text{H}_{11}\text{O}_3\text{N}$ | 3410 | 1620 | 1680 | 1320 | - | - |
| $[\text{CoC}_{28}\text{H}_{18}\text{O}_6\text{N}_2]\cdot 2\text{H}_2\text{O}$ | 3436 | 1541 | 1598 | 1305 | 590 | 457 |

301

302 3.4.3 IR spectra of Schiff Base ligand $\text{C}_9\text{H}_{11}\text{N}_3\text{OS}$ (L^3) and Its metal complex

303 a. IR-Spectra of Schiff base $\text{C}_9\text{H}_{11}\text{N}_3\text{OS}$ (L^3)

304 The peaks obtained at 3406cm^{-1} and 3291cm^{-1} may be assigned to symmetric and asymmetric
 305 $\nu(-\text{N-H})$ stretching frequency of primary amino group. The broad peak obtained between
 306 3282 and 2829cm^{-1} may be assigned to overlapping of peaks of hydrogen bonded $\nu(\text{N-H})$
 307 and aromatic C-H stretching frequency. The bands obtained between 1183cm^{-1} and 1252cm^{-1}
 308 1 in ligand were due to $\nu(-\text{OCH}_3)$ groups (figure-18). The peaks observed at 1606cm^{-1} and 834
 309 cm^{-1} may be assigned to $\nu(\text{C=N})$ and $\nu(\text{C=S})$ [37-39].



310

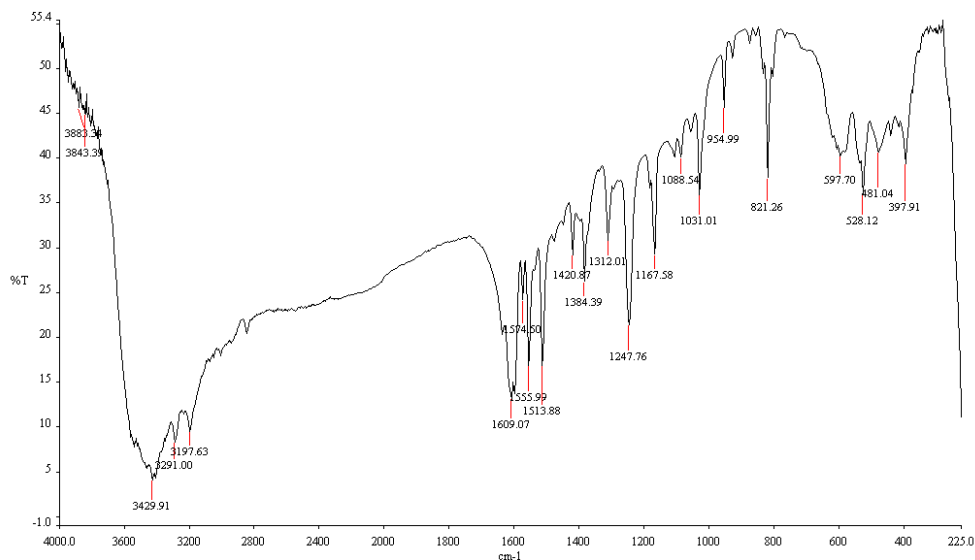
Figure-18: IR Spectra of Schiff base ligand $C_9H_{11}N_3OS$ (L^3)

311

312 **b. IR-Spectra of $[C_{18}H_{22}CdO_2N_6S_2]$ with ligand (L^3)**

313 The bands at 1606 cm^{-1} and 834 cm^{-1} assigned to $\nu(C=N)$ and $\nu(C=S)$ modes and these bands
 314 shifted towards lower frequency in the spectra of Cd(II) complex (figure-19), which indicated
 315 that coordination takes place through nitrogen of $\nu(C=N)$ group and sulphur of $\nu(C=S)$ group.
 316 At lower frequency the complex exhibited new bands at 540 and 397 cm^{-1} which further
 317 supported the coordination site $\nu(M-N)$ and $\nu(M-S)$ vibrations.

318



319

Figure-19: IR Spectra of $[CdC_{18}H_{22}O_2N_6S_2]$

320

321 **Table-5:** FTIR spectral data of the ligand L³ and its Cd(II) metal complex (in cm⁻¹)

| Ligand / Metal Complexes | IR/cm ⁻¹ | | | |
|--|---------------------|--------|--------|--------|
| | v(C=N) | v(C=S) | v(M-N) | v(M-S) |
| Ligand (L ³) C ₉ H ₁₁ N ₃ OS | 1606 | 834 | - | - |
| [Cd(L ³) ₂] [CdC ₁₈ H ₂₂ O ₂ N ₆ S ₂] | 1574 | 821 | 528 | 397 |

322

323 3.5 Characterization by UV-visible Spectra

324 a. UV-vis spectra and magnetic moment of Zn(II) complex with ligand C₈H₉ON₃S (L¹)

325 The electronic spectral data for the ligand and their metal complex recorded in DMSO are
 326 summarized in Table-6. There are two absorption bands, assigned to n-π* and π-π*
 327 transitions, in the electronic spectrum of the ligand. These transitions are also found in the
 328 spectra of the complexes, but they are shifted towards lower and higher frequencies,
 329 indicating the coordination of the ligand to the metallic ions [40]. The UV spectra of the
 330 ligand shows three absorption bands at 260nm,310nm and 355nm.The first two bands are
 331 assigned to π-π* transitions of azomethine chromospheres and a benzene ring and the third is
 332 assigned to n-π* transition of a lone pair of electrons of an azomethine nitrogen and an
 333 antibonding π orbital. The absorption band n-π*at 355 nm due to an imine group in the
 334 ligand, whereas for the zinc complex, the same was observed at 390 nm with weak absorption
 335 intensity which indicate the coordination of zinc with imine group [41]. The zinc complex
 336 shows only the charge transfer transition which can be assigned to charge transfer from the
 337 ligand to the metal and vice versa, no d-d transitions are expected for d¹⁰ Zn(II) complex [42].

338 b. UV-vis spectra and magnetic moment of Ni(II) complex with ligand C₈H₉ON₃S (L¹)

339 The UV-Vis absorption spectra of the ligand and complex were recorded after dissolving into
 340 DMSO solvent at room temperature. There are two absorption bands, assigned to n-π* and
 341 π-π* transitions, in the electronic spectrum of the ligand. These transitions are also found in
 342 the spectra of the complexes, but they are shifted towards lower and higher frequencies,
 343 confirming the coordination of the ligand to the metallic ions [43]. The electronic spectrum of
 344 ligand exhibits three intense absorption peaks at 260 nm, 310 nm and 350nm.The first and
 345 second peaks were attributed to benzene π-π*and imino π-π*transitions and the third peak in

346 the spectra was assigned to $n-\pi^*$ transition [44]. The electronic spectra of the Ni(II) complex
347 with an electronic configuration of d^8 shows three new absorption bands in the visible region
348 and these three bands of the transitions $^1A_{1g} \rightarrow ^1A_{2g}$ (355nm), $^1A_{1g} \rightarrow ^1B_{1g}$ (380nm) and
349 $^1A_{1g} \rightarrow ^1E_g$ (420 nm) were observed in the spectra of a square-planar Ni(II) complex [45,46].

350 **c. UV-vis spectra and magnetic moment of Mn(II) complex with ligand $C_8H_9ON_3S$ (L^1)**

351 The UV-Vis absorption spectra of the ligand and complex were recorded after dissolving into
352 DMSO solvent at room temperature. There are two absorption bands, assigned to $n-\pi^*$ and
353 $\pi-\pi^*$ transitions, in the electronic spectrum of the ligand. These transitions are also found in
354 the spectra of the complexes, but the ligand to the metallic ions [47]. The electronic spectrum
355 of ligand exhibits three intense absorption peaks at 260 nm, 310 nm and 350nm. The first and
356 second peaks were attributed to benzene $\pi-\pi^*$ and imino $\pi-\pi^*$ transitions and the third peak in
357 the spectra was assigned to $n-\pi^*$ transition. Due to Forbidden transition, several bands were
358 observed in the visible region of Mn(II) complex, and the band at 430 nm is attributed to (d-
359 d) transition of type $^6A_1 \rightarrow ^4T_2$.

360 **d. UV-vis spectra and magnetic moment of Sn(II) complex with ligand $C_8H_9ON_3S$ (L^1)**

361 The electronic absorption spectra of ligand L^1 and its Sn (II) complex in DMSO solution
362 were carried out in the range of 200-800 nm at room temperature. There is a shift of the
363 bands to longer wave length in spectra of complex is a good evidence of complex formation.
364 There were various bands in the ligand spectra assigned to inter ligand and charge transfer of
365 $n-\pi^*$ transitions according to their energies and intensities. Ligand exhibits three intense
366 absorption peaks at 260 nm, 310 nm and 350nm. The first and second peaks were attributed to
367 benzene $\pi-\pi^*$ and imino $\pi-\pi^*$ transitions and the third band in the spectra was assigned to $n-$
368 π^* transition. The complex showed an intense band at 410nm due to the $n-\pi^*$ transition of
369 azomethine chromosphere and the band at 340 nm may be assigned as charge transfer band. It
370 has been reported that the metal is capable of forming $dn-p\pi^*$ bonds with ligands containing
371 nitrogen as the donor atom. The Sn atom has its 5d orbital completely vacant and hence
372 $Sn \leftarrow N$ bonding can take place by the acceptance of the lone pair of electrons from the
373 azomethine nitrogen of the ligand [48-50].

374

375

376 **Table-6:** Magnetic moments and electronic spectral data for ligand (L¹) and its metal
 377 complexes

| Compound | λ_{\max} n.m | Wave number cm ⁻¹ | μ_{eff} B.M | Assignment |
|---|-------------------------|---------------------------------|---------------------------|---------------------------------|
| C ₈ H ₉ ON ₃ S | 260 | 38461 | - | $\pi \rightarrow \pi^*$ |
| | 310 | 32258 | | $\pi \rightarrow \pi^*$ |
| | 350 | 38571 | | $n \rightarrow \pi^*$ |
| [NiC ₁₆ H ₁₆ O ₂ N ₆ S ₂].H ₂ O | 355 | 28169 | 1.469 | $^1A_{1g} \rightarrow ^1A_{2g}$ |
| | 380 | 26315 | | $^1A_{1g} \rightarrow ^1B_{1g}$ |
| | 420 | 23809 | | $^1A_{1g} \rightarrow ^1E_g$ |
| [ZnC ₁₆ H ₁₆ O ₂ N ₆ S ₂].2H ₂ O | 265 | 37735 | 0.5197 | C.T (M→L) |
| | 320 | 31250 | | C.T (M→L) |
| | 390 | 25641 | | C.T (M→L) |
| [MnC ₁₆ H ₁₆ O ₂ N ₆ S ₂].H ₂ O | 325 | 30769 | 2.507 | $^6A_1 \rightarrow ^4T_2$ |
| | 380 | 26315 | | |
| | 430 | 23255 | | |

378

379 **e. UV-vis spectra and magnetic moment of Co(II) complex with ligand C₁₄H₁₁O₃N (L²)**

380 The magnetic moment and electronic spectra are very effective in the evaluation of results
 381 obtained by other methods of structural investigation. Information regarding the geometry of
 382 the complex of Co(II) ions was obtained from electronic spectral studies and magnetic
 383 moments (table-7). The electronic spectra of ligand and their metal complexes were recorded
 384 in DMSO. Electronic spectrum of ligand shows strong absorption band at 330nm region can
 385 be assigned to the $n \rightarrow \pi^*$ transition of the azomethine group of ligand, which slightly shifted
 386 to lower frequency in the spectra of the complex, indicating that the azomethine nitrogen
 387 atom is involved in coordination to the metal ion. The Co(II) complex was found the
 388 magnetic moment 4.0137 B.M which indicated the three unpaired electrons per Co(II) ion
 389 attaining an octahedral environment [60]. The electronic spectrum of Co(II) complex shows
 390 bands at 264nm and 274nm are assignable to metal-ligand charge transfer band and the band
 391 400nm is assignable to $^4T_{1g}(F) \rightarrow ^4T_{1g}(P)$ transition.

392

393 **Table-7:** The electronic spectral data and magnetic moments for ligand (L²) and it's metal
 394 complex

| Compound | λ_{\max} n.m | Wave number cm ⁻¹ | μ_{eff} B.M | Assignment |
|--|-------------------------|---------------------------------|---------------------------|--|
| C ₁₄ H ₁₁ O ₃ N | 330 | 30303 | - | n→ π^* |
| [CoC ₂₈ H ₁₈ O ₆ N ₂].2H ₂ O | 264 | 37878 | 4.0137 | Charge transfer(C.T) |
| | 274 | 36496 | | C.T (M→L) |
| | 400 | 25000 | | ⁴ T _{1g} (F)→ ⁴ T _{1g} (P) |

395

396 **f. UV-vis spectra and magnetic moment of Cd(II) complex with ligand C₉H₁₁N₃OS (L³)**

397 The electronic spectral data for the ligand and it's metal complex recorded in DMSO are
 398 summarized in Table-8. There are two absorption bands, assigned to n- π^* and π - π^*
 399 transitions, in the electronic spectrum of the ligand. These transitions are also found in the
 400 spectra of the complexes, but they are shifted towards lower and higher frequencies,
 401 indicating the coordination of the ligand to the metallic ions. The UV spectra of the ligand
 402 shows three absorption bands at 280nm,330nm and 350nm.The first two bands are assigned
 403 to π - π^* transitions of azomethine chromospheres and a benzene ring and the third is assigned
 404 to n- π^* transition of a lone pair of electrons of an azomethine nitrogen and an anti-bonding π
 405 orbital. The absorption band n- π^* at 350nm due to an imine group in the ligand, whereas for
 406 the Cd(II) complex, the same was observed at 400 nm with weak absorption intensity which
 407 indicate the coordination of cadmium with imine group. The cadmium complex show only
 408 the charge transfer transition which can be assigned to charge transfer from the ligand to the
 409 metal and vice versa, no d-d transition are expected for diamagnetic d¹⁰ Cd(II) complex. The
 410 shifting of ligand absorption in the UV region, in the spectra of the complex confirming the
 411 coordination of the ligand to metal like Cd (II) ions.

412

413

414

415

416 **Table-8:** Magnetic moments and electronic spectral data for ligand (L^3) and it's Cd(II)
 417 Complex

| Compound | λ_{\max} n.m | Wave number cm^{-1} | μ_{eff} B.M | Assignment |
|--|-------------------------|---------------------------------|---------------------------|-------------------------|
| $\text{C}_9\text{H}_{11}\text{N}_3\text{OS}$ | 280 | 35714 | - | $\pi \rightarrow \pi^*$ |
| | 330 | 30303 | | $\pi \rightarrow \pi^*$ |
| | 350 | 28571 | | $n \rightarrow \pi^*$ |
| [$\text{CdC}_{18}\text{H}_{22}\text{O}_2\text{N}_6\text{S}_2$] | 295 | 33898 | 0.4606 | C.T (M \rightarrow L) |
| | 340 | 29412 | | C.T (M \rightarrow L) |
| | 400 | 25000 | | C.T (M \rightarrow L) |

418

419 3.6 Characterization by Thermogravimetric Analysis

420 Thermogravimetric analysis of Zn(II),Ni(II),Mn(II) and Sn(II) complexes of ligand 421 $\text{C}_8\text{H}_9\text{ON}_3\text{S}$ (L^1)

422 The thermal decomposition analysis of solid Zn(II), Ni(II), Mn(II) and Sn(II) metal
 423 complexes were carried out under nitrogen atmosphere and heating rate was suitably
 424 controlled at $30^\circ\text{C min}^{-1}$ and the weight loss was measured from the ambient temperature up
 425 to 800°C .The data from TGA and DTG clearly indicated that the decomposition of the
 426 complexes proceed in three or four steps. There were some minor steps and asymmetry of
 427 TGA/DTG curves also observed. The weight losses for each complex were calculated within
 428 the corresponding temperature ranges. The different thermodynamic parameters are listed in
 429 Table-9.

430 a. For [$\text{ZnC}_{16}\text{H}_{16}\text{O}_2\text{N}_6\text{S}_2$]. $2\text{H}_2\text{O}$ Complex

431 The TGA and DTG curve of Zn(II) complex shown in (figure-20), indicated that the complex
 432 was decomposed into four main steps. In the first step of decomposition, two molecules of
 433 water were lost at the temperature range of $85\text{-}110^\circ\text{C}$ (calculated 7.36%, experimental
 434 7.20%). In this temperature range the loss of water molecules indicates that the water
 435 molecules are of lattice type [51,52].In the temperature range $130\text{-}335^\circ\text{C}$ (calculated 24.00%
 436 and experimental 23.10%), the part of ligand- 2CSNH_2 were decomposed at the second step.
 437 The other part of the ligand $2\text{C}_6\text{H}_4\text{O}$ - were decomposed in third step at $335\text{-}740^\circ\text{C}$ (calculated
 438 37.50%, experimental 32 .00%). At above 750°C temperature the complex was decomposed

439 and removed as Zn/ZnO (calculated 31.14%, experimental 37.70%) polluted with few carbon
440 atoms [53].

441 **b. For $[\text{NiC}_{16}\text{H}_{16}\text{O}_2\text{N}_6\text{S}_2]\cdot\text{H}_2\text{O}$ Complex**

442 The TGA and DTG curve of Ni(II) complex shown in (figure-21) that the complex was
443 decomposed into four main steps. The 1st step involves the removal of one molecule of
444 hydrated water (calculated 3.87%, experimental 4.00% weight) at temperature range 80-
445 190°C [54,55]. In the 2nd step the part of the ligand $2\text{C}_6\text{H}_4\text{O}^-$ was decomposed at 280-350°C
446 (calculated 39.59%, experimental 34.82% weight). At the 3rd step the fragmentation of
447 coordinated ligand $2\text{C}_2\text{H}_4\text{N}_3\text{S}$ was decomposed from the complex at the temperature range
448 360-750°C (calculated 43.90%, experimental 44.20% weight) and above 750°C temperature
449 the complex was completely decomposed and removed as Ni/NiO (calculated 12.64%,
450 experimental 16.98%).

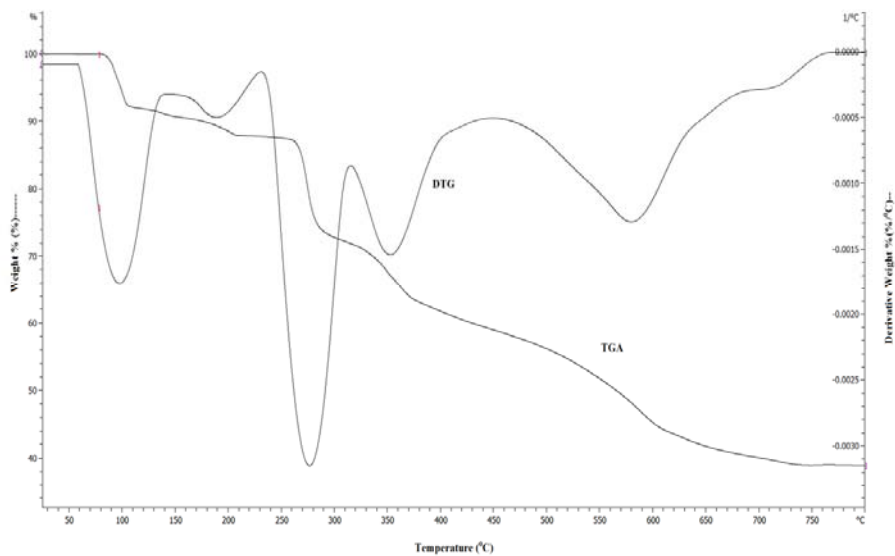
451 **c. For $[\text{MnC}_{16}\text{H}_{16}\text{O}_2\text{N}_6\text{S}_2]\cdot\text{H}_2\text{O}$ Complex**

452 In the case of Mn(II) complex the TGA and DTG curve indicated in (figure-22) that the
453 complex was decomposed into four main steps. At 1st step one molecule of hydrated water
454 was removed at 80-180°C (calculated 3.90%, experimental 4.00%) [54,55]. Then the
455 dehydrated complex was gradually decomposed and the part of ligand $2\text{C}_6\text{H}_4\text{O}^-$ was removed
456 at the temperature range 180-350°C (calculated 39.92%, experimental 38.10%). The 3rd step
457 involves the decomposition of the ligand part $2\text{CH}_3\text{N}_2\text{S}$ at the temperature range 350-
458 770°C (calculated 32.54%, experimental 32.22%). At above 770°C temperature finally the
459 complex was completely decomposed and removed as Mn/MnO (calculated 23.64%,
460 experimental 25.68%).

461 **d. For $[\text{SnC}_{16}\text{H}_{16}\text{O}_2\text{N}_6\text{S}_2]$ Complex**

462 The Sn(II) complex showed high thermal stability and decomposed above 170 °C, indicating
463 the absence of any lattice water molecules [69]. This complex was decomposed into four main
464 steps shown in (figure-23). At first step the part of ligand $(-2\text{CH}_2\text{NS})$ were decomposed
465 at temperature 170-275°C (calculated 23.67%, experimental 22.00%). In 2nd step the
466 decomposition of $(-2\text{CHN}-)$ moiety was take place at temperature 275-330°C (calculated
467 12.0%, experimental 10.65 %). The ligand part $(2\text{C}_6\text{H}_4\text{O}^-)$ were decomposed at the 3rd step at
468 temperature range 330-750°C (calculated 36.29%, experimental 36.10 %) and finally the

469 complex was completely decomposed and removed as Sn/SnO (calculated 28.04%,
470 experimental 31.25%).

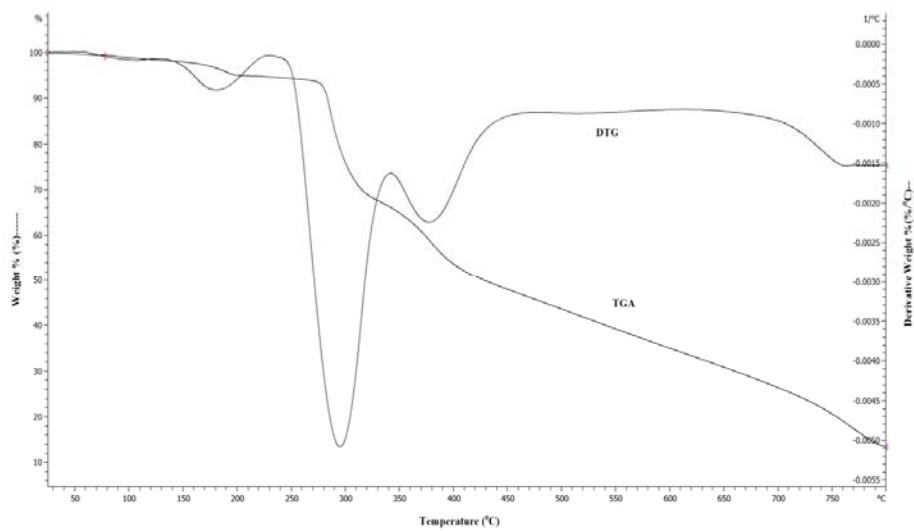


471

472 Figure-20: TGA and DTG curve of [ZnC₁₆H₁₆O₂N₆S₂].2H₂O

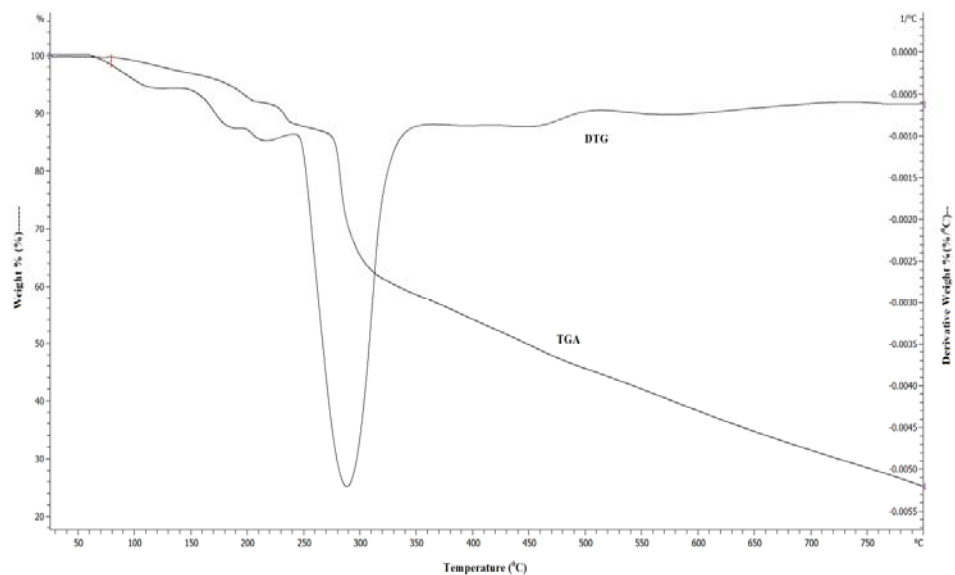
473

474



475

476 Figure-21: TGA and DTG curve of [NiC₁₆H₁₆O₂N₆S₂].H₂O

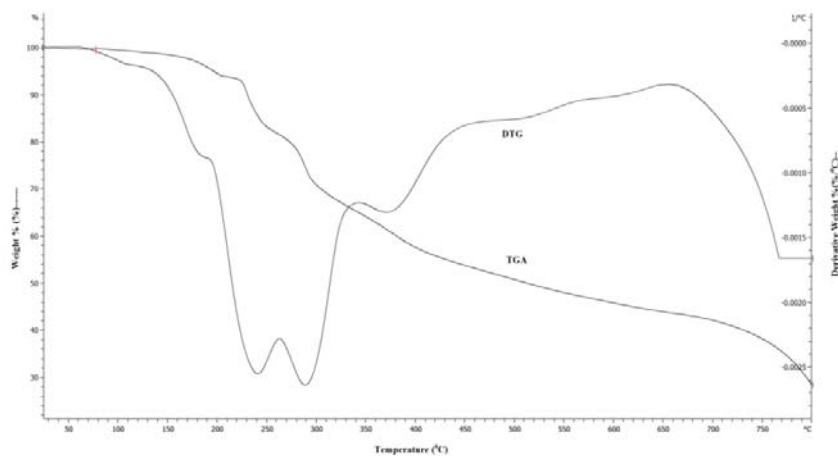


477

478

Figure-22: TGA and DTG curve of $[\text{MnC}_{16}\text{H}_{16}\text{O}_2\text{N}_6\text{S}_2]\cdot\text{H}_2\text{O}$

479



480

481

Figure-23: TGA and DTG curve of $[\text{SnC}_{16}\text{H}_{16}\text{O}_2\text{N}_6\text{S}_2]$

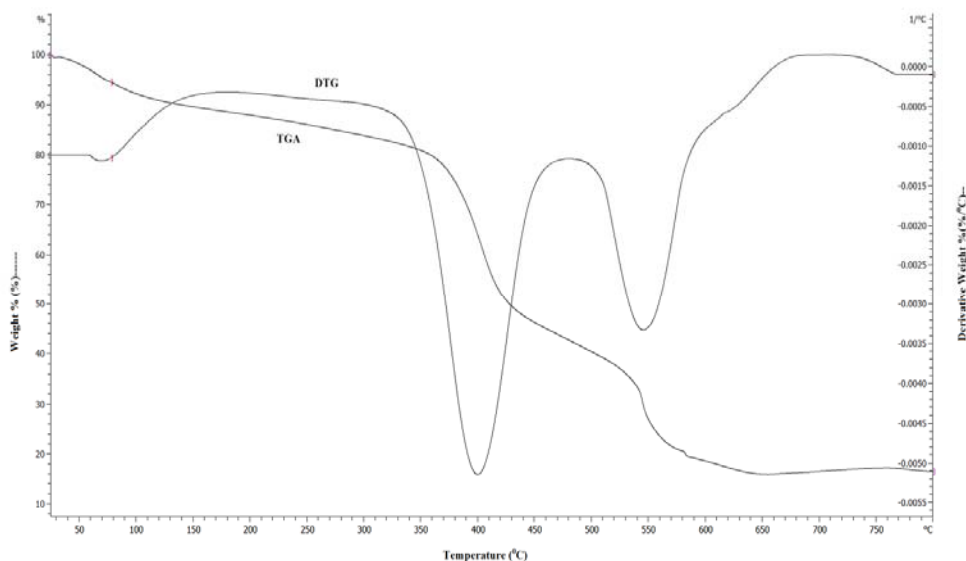
482 **Table- 9:** Thermal data of Zn(II), Ni(II), Mn(II) and Sn(II) complexes of ligand $\text{C}_8\text{H}_9\text{ON}_3\text{S}$
 483 (L^1)

| Complexes | Steps | Temperature Range/ °C | DTG Peak/ °C | TG mass loss% calc./found | Assignments |
|-----------|-------|-----------------------|--------------|---------------------------|-------------|
|-----------|-------|-----------------------|--------------|---------------------------|-------------|

| | | | | | |
|---|-----------------|---------|-----|-------------|---|
| [ZnC ₁₆ H ₁₆ O ₂ N ₆ S ₂].2H ₂ O | 1 st | 85-110 | 97 | 7.36/7.20 | 2H ₂ O |
| | 2 nd | 130-335 | 278 | 24.00/23.10 | 2CSNH ₂ |
| | 3 rd | 335-740 | 350 | 37.50/32.00 | 2C ₆ H ₄ O- |
| | 4 th | >750 | | 31.14/37.7 | Zn/ZnO |
| [NiC ₁₆ H ₁₆ O ₂ N ₆ S ₂].H ₂ O | 1 st | 80-190 | 180 | 3.87/4.00 | H ₂ O |
| | 2 nd | 280-350 | 295 | 39.59/34.82 | 2C ₆ H ₄ O ⁻ |
| | 3 rd | 360-750 | 382 | 43.90/44.20 | 2C ₂ H ₄ N ₃ S |
| | 4 th | >750 | | 12.64/16.98 | Ni/NiO |
| [MnC ₁₆ H ₁₆ O ₂ N ₆ S ₂].H ₂ O | 1 st | 80-180 | 118 | 3.90/4.00 | H ₂ O |
| | 2 nd | 180-350 | 290 | 39.92/38.10 | 2C ₆ H ₄ O ⁻ |
| | 3 rd | 350-770 | | 32.54/32.22 | 2CH ₃ N ₂ S |
| | 4 th | >770 | | 23.64/25.68 | Mn/MnO |
| [SnC ₁₆ H ₁₆ O ₂ N ₆ S ₂] | 1 st | 170-275 | 240 | 23.67/22.00 | 2CH ₂ NS |
| | 2 nd | 275-330 | 290 | 12.00/10.65 | 2CHN- |
| | 3 rd | 330-750 | 370 | 36.29/36.10 | 2C ₆ H ₄ O ⁻ |
| | 4 th | >750 | | 28.04/31.25 | Sn/SnO |

484 **Thermogravimetric analysis of Co(II) complex of ligand C₁₄H₁₁O₃N (L²)**

485 TGA was carried out for solid Co(II) metal complex under N₂ flow. The heating rate was
486 suitably controlled at 30°C min⁻¹ and the weight loss was measured from the ambient
487 temperature up to 800°C. The thermogram of complex exhibits three clear cut decomposition
488 stages in (figure-24). The first stage with estimated mass loss of 6.32% (calculated mass loss
489 6.28%) within the temperature range 40–110°C corresponding to the loss of water molecules
490 [56,57]. The second stage occurs at 110–480°C, with a mass loss of 49.20% (calculated
491 51.31%) , corresponding to the loss of 2C₈H₅O₂N parts of the ligand. The third stage of
492 decomposition occurs at the temperature range 480–650°C, with a mass loss of 28.80%
493 (calculated 32.12%), corresponding to the loss of 2C₆H₄O moiety. At above 650°C
494 temperature the complex was completely decomposed and removed as of 15.72% (calculated
495 10.29%). The different TG and DTG data are given in Table-10.



496

497

Figure-24: TGA and DTG curve of $[\text{CoC}_{28}\text{H}_{18}\text{O}_6\text{N}_2].2\text{H}_2\text{O}$

498

Table- 10: Thermal data of Co(II) complex of ligand $\text{C}_{14}\text{H}_{11}\text{O}_3\text{N}$ (L^2)

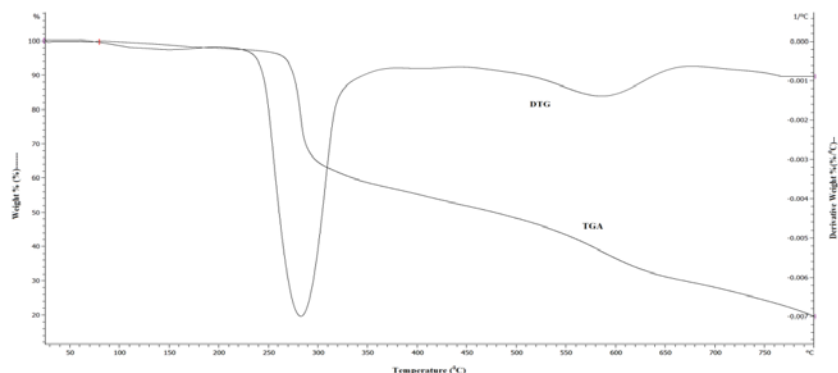
| Complexes | Steps | Temperature Range/ °C | DTG Peak/ °C | TG mass loss% calc./found | Assignments |
|--|-----------------|-----------------------|--------------|---------------------------|---|
| $[\text{CoC}_{28}\text{H}_{18}\text{O}_6\text{N}_2].2\text{H}_2\text{O}$ | 1 st | 40-110 | 65 | 6.28/6.32 | $2\text{H}_2\text{O}$ |
| | 2 nd | 110-480 | 400 | 51.31/49.20 | $2\text{C}_8\text{H}_5\text{O}_2\text{N}$ |
| | 3 rd | 480-650 | 548 | 32.12/28.80 | $2\text{C}_6\text{H}_4\text{O}^-$ |
| | 4 th | >650 | | 10.29/15.72 | Co/CoO |

499

500 **Thermogravimetric analysis of Cd(II) complex of ligand $\text{C}_9\text{H}_{11}\text{N}_3\text{OS}$ (L^3)**

501 Thermogravimetric analysis of solid Cd(II) metal complex under N_2 flow. The heating rate
 502 was suitably controlled at $30^\circ\text{C min}^{-1}$ and the weight loss was measured from the ambient
 503 temperature up to 800°C . The TGA curve of the Cd(II) complex showed no mass loss up to
 504 230°C , indicating the absence of lattice / coordinated water [58,59] and the high thermal
 505 stability of the complex. The thermogram of Cd(II) complex is given in Fig.4.24, which
 506 shows two stage decomposition pattern. The first stage was exhibited a maximum mass loss
 507 of 49.23% (calculated 50.53%) of ligand part ($2\text{C}_8\text{H}_8\text{ON}$) at $230\text{--}455^\circ\text{C}$. The second stage
 508 occurs at $455\text{--}740^\circ\text{C}$, with a mass loss of 27.05% (calculated 28.28%) attributed to the loss
 509 of ($2\text{CH}_3\text{N}_2\text{S}$) moiety. Finally at above 750°C temperature the complex was completely

510 decomposed and removed as Cd/CdO of 24.0% (calculated 21.19%). The different TG and
 511 DTG data are given in Table-11.



512

513 Figure-25: TGA and DTG curve of $[CdC_{18}H_{22}O_2N_6S_2]$

514

Table- 11: Thermal data of Cd(II) complex of ligand $C_9H_{11}N_3OS (L^3)$

515

| Complexes | Steps | Temperature Range/ °C | DTG Peak/ °C | TG mass loss% calc./found | Assignments |
|-----------------------------|-----------------|-----------------------|--------------|---------------------------|-------------|
| $[CdC_{18}H_{22}O_2N_6S_2]$ | 1 st | 230-455 | 282 | 50.53/49.23 | $2C_8H_8ON$ |
| | 2 nd | 455-740 | 570 | 28.28/27.05 | $2CH_3N_2S$ |
| | 3 rd | >740 | | 21.19/24.00 | Cd/CdO |

516

516 Antibacterial activity

517 The prime objective of performing the antibacterial screening is to determine the
 518 susceptibility of the pathogenic microorganism to test the compound which, in turn is used to
 519 selection of the compound as a therapeutic agent. The free Schiff base ligand and their metal
 520 complexes were screened for their antibacterial activity against strains the *Bacillus cereus*
 521 *ATCC25923*, *Streptococcus agalactiae*, *Escherichia coli ATCC 25922*, *Shigella dysenteriae*
 522 The compounds were tested at a concentration of 30 μ g/0.01 mL in DMSO solution using the
 523 paper disc diffusion method with Kanamycin as standard. The susceptibility zones were
 524 measured in diameter (mm) and the result are listed in Table-12. The susceptibility zones
 525 were the clear zones around the discs killing the bacteria.

526

527

528 **Table 12.** Antibacterial activities of the complexes.

| Bacterials strains | Zone of inhibition, diameter in mm | | | | | | |
|---------------------------------|------------------------------------|-------------------|-------------------|-------------------|-------------------|-------------------|-------------------|
| | A (10µg /disc) | B (10µg /disc) | C (10µg /disc) | D (10µg /disc) | E (10µg /disc) | F (10µg /disc) | K (30µg /disc) |
| Gram positive | | | | | | | |
| <i>Bacillus cereus</i> | 22 | 10 | 19 | 12 | 11 | 14 | 36 |
| <i>Streptococcus agelactiae</i> | 19 | 09 | 21 | 08 | 14 | 16 | 35 |
| Gram negative | | | | | | | |
| <i>Escherichia coli</i> | 23 | 12 | 24 | 09 | 12 | 18 | 32 |
| <i>Shigella dysenteriae</i> | 09 | 11 | 10 | 12 | 08 | 14 | 36 |

529

530 Where, A = $[C_{16}H_{16}ZnO_2N_6S_2].2H_2O$, B = $[C_{16}H_{16}NiO_2N_6S_2].H_2O$, C = $[C_{16}H_{16}MnO_2N_6S_2].H_2O$, D =
531 $[C_{16}H_{16}SnO_2N_6S_2]$, E = $[C_{28}H_{18}CoO_6N_2].2H_2O$, F = $[C_{18}H_{22}CdO_2N_6S_2]$ and K = Kanamycin

532 **Conclusion**

533 In this paper we have explored the synthesis and coordination Chemistry of Ni(II), Zn(II),
534 Mn(II), Sn(II), Co(II) and Cd(II) ions were synthesized with three different synthesized
535 Schiff base ligands viz (L¹) [2-(2-hydroxybenzylidene)hydrazinecarbothioamide, (L²) [4-((4-
536 hydroxybenzylidene)amino)benzoic acid and (L³) [2-(4-
537 methoxybenzylidene)hydrazinecarbothioamide]. The ligands and metal complexes were
538 characterized by molar conductivity measurement, magnetic susceptibility, Infrared,
539 electronic spectral, thermal analysis and some physical measurements. The overall reactions
540 were monitored by TLC analysis. Molar conductance study have shown that all the
541 complexes were non electrolytic in nature. FTIR studies suggested that Schiff bases act as
542 deprotonated bidentate ligands and metal ions are attached with the ligands-(L¹), (L²) by N, O

543 and ligand-(L³) by N, S coordinating sites during complexation reaction. Magnetic
544 susceptibility data coupled with electronic spectra revealed that [ZnC₁₆H₁₆O₂N₆S₂].2H₂O,
545 [MnC₁₆H₁₆O₂N₆S₂].H₂O, [SnC₁₆H₁₆O₂N₆S₂] and [CdC₁₈H₂₂O₂N₆S₂] complexes have tetrahedral,
546 [NiC₁₆H₁₆O₂N₆S₂].H₂O has square planer and [CoC₂₈H₁₈O₆N₂].2H₂O has octahedral geometry.
547 Thermal analysis (TGA and DTG) data showed the possible degradation pathway of the
548 complexes and also indicated that most of the complexes were thermally stable up to 200⁰C.
549 The Schiff bases and their metal complexes have been found moderate to strong
550 antimicrobial activity.

551 REFERENCES

- 552 [1]. Angela Kriza, Lucica Viorica Ababei, Nicoleta Cioatera, Ileana Rău And Nicolae
553 Stănică, Synthesis And Structural Studies Of Complexes Of Cu, Co, Ni And Zn With
554 Isonicotinic Acid Hydrazide And Isonicotinic Acid (1-Naphthylmethylene)Hydrazide,
555 J. Serb. Chem. Soc., 2010,75 (2), 229- 242.
- 556 [2]. P. K. Das, N. Panda, N. K. Behera, Synthesis, Characterization and Antimicrobial
557 Activities of Schiff Base Complexes Derived from Isoniazid and Diacetylmonoxime,
558 IJISSET - International Journal of Innovative Science, Engineering & Technology,
559 2016, 3(1), 42-54.
- 560 [3]. Anil Kumar M R, Shanmukhappa S, Rangaswamy B E, Revanasiddappa M,
561 Synthesis, Characterization, Antimicrobial Activity, Antifungal Activity and DNA
562 Cleavage Studies of Transition Metal Complexes with Schiff Base Ligand,
563 International Journal of Innovative Research in Science, Engineering and Technology,
564 2015,4(2), 60-66.
- 565 [4]. O' Boyle N M, Tenderholt A L & Langer K M, cclib: a library for package-
566 independent computational chemistry algorithms J. Comput. Chem., 2008, 29, 839.
- 567 [5]. Saud I. Al-Resayes, Mohammad Shakir, Ambreen Abbasi, Kr. Mohammad Yusuf
568 Amin, Abdul Lateef, Synthesis, spectroscopic characterization and biological
569 activities of N4O2 Schiff base ligand and its metal complexes of Co(II), Ni(II), Cu(II)
570 and Zn(II), Spectromica Acta Part A , 2012, 93, 86-94.
- 571 [6]. K.D. Karlin, Z. Tyeklar, Bioinorganic Chemistry of Copper, Chapman & Hall: New
572 York, 1993, 101-109.
- 573 [7]. V. Arun, N. Sridevi, P.P. Robinson, S. Manju, K.K.M. Yusuff, "Ni(II) and Ru(II)
574 Schiff base complexes as catalysts for the reduction of benzene" J. Mol. Catal. A:
575 Chem., 2009, 304 (1-2), 191-198.

- 576 [8]. K. C. Gupta, A. K. Sutar, Catalytic activities of Schiff base transition metal
577 complexes, *Coord. Chem. Rev.*, 2008, 252 (12-14), 1420-1450.
- 578 [9]. R. I. Kureshy, N. H. Khan, S. H. R. Abdi, P. Iyer and S. T. Patel, Chiral Ru(II) Schiff
579 base complexes catalysed enantio selective epoxidation of styrene derivatives using
580 iodobenzene as oxidant II, *J. Mol. Catal.*, 1999, 150(1-2), 175-183.
- 581 [10]. Saud I. Al-Resayes, Mohammad Shakirb, Ambreen Abbasi, Kr. Mohammad Yusuf
582 Amin, Abdul Lateef, *Spectromica Act.a Part A*, 2012, 93, 86-94.
- 583 [11]. Rakesh Ranjan and Dhanashree S Hallooman, Synthesis And Characterization Of
584 Co(II) And Ni(II) Complexes With Schiff Base 2,2-
585 Dimethylpropionophenonethiosemicarbazone, *International Journal Of Research In
586 Pharmacy And Chemistry*, 2014, 4(2), 423-426.
- 587 [12]. Angela Kriza, Mariana Loredana Dianu, Nicolae Stănică, Constantin Drăghici, Mona
588 Popoiu, Synthesis and Characterization of Some Transition Metals Complexes with
589 Glyoxalbis- Isonicotinoyl Hydrazone, 2009, 60(6), 555-560.
- 590 [13]. L. Mitu, A. Kriza, Synthesis and Characterization of Complexes of Mn(II), Co(II),
591 Ni(II) and Cu(II) with an Aroylhydrazone Ligand. *Asian J. Chem.*, 2007, 19 (1), 658-
592 664.
- 593 [14]. Ljubijankić N., Tešević V., Grgurić-Šipka S., Jadranin M., Begić S., Buljubašić L.,
594 Markotić E., Ljubijankić S., Synthesis and characterization of Ru(III) complexes with
595 thiosemicarbazide-based ligands, 2016, 47, 1-6.
- 596 [15]. Methak. S. Mohammad, Preparation and Characterization of Some Transition Metal
597 Complexes with Schiff base of thiosemicarbazone, *Journal of Kerbala University,
598 Scientific*. 2010, 8 (1), 8-17 .
- 599 [16]. R.V. Singh, N. Fahmi and M.K. Biyala, Coordination Behavior and Biopotency of N
600 and S/O Donor Ligands with their Palladium(II) and Platinum(II) Complexes, *Journal
601 of the Iranian Chemical Society*, 2005, 2(1), 40-46.
- 602 [17]. A. M. Vijey, G. Shiny, and V. Vaidhyalingam, Synthesis and antimicrobial activities
603 of 1-(5-substituted-2-oxo indolin-3-ylidene)-4-(substituted pyridin-2-yl)
604 thiosemicarbazide, *Arkivoc (xi)*., 2008, 187.
- 605 [18]. Mohammad Asif, A Review On Biological Activities Of Benzimidazole, Oxadiazole
606 And Mannich Base Derivatives Of Benzimidazole-Oxadiazole Merged Compounds,
607 *International Journal of Current Research in Applied Chemistry & Chemical
608 Engineering*, 2017, 3(1), 20-29.

- 609 [19]. M. M. H. Khalil, M. M. Aboaly and R. M. Ramadan, Spectroscopic and
610 electrochemical studies of ruthenium and osmium complexes of salicylideneimine-2-
611 thiophenol Schiff base, 2005, 61(1), 157-161.
- 612 [20]. P. M. Dahikar, R. M. Kedar, Synthesis, spectral and biological activity of transition
613 metal complexes of substituted benzoinsemicarbazones, International Journal of
614 Application or Innovation in Engineering & Management (IJAEM), 2013, 2(4), 8-11.
- 615 [21]. P. Murali Krishna, B. S. Shankara, and N. Shashidhar Reddy, Synthesis,
616 Characterization, and Biological Studies of Binuclear Copper(II) Complexes of (2E)-
617 2-(2-Hydroxy-3-Methoxybenzylidene)-4N-Substituted Hydrazine carbothioamides,
618 Hindawi Publishing Corporation, International Journal of Inorganic Chemistry,
619 2013, 11 pages.
- 620 [22]. Ljiljana S. Vojinović-Ješić, Vukadin M. Leovac, Mirjana M. Lalović, Valerija I.
621 Češljević, Ljiljana S. Jovanović, Marko V. Rodić and Vladimir Divjaković, Transition
622 metal complexes with thiosemicarbazide-based ligands. Part 58. Synthesis, spectral
623 and structural characterization of dioxovanadium(V) complexes with
624 salicylaldehydethiosemicarbazone, J. Serb. Chem. Soc. 2011, 76 (6), 865–877.
- 625 [23]. Monika Tyagi, Sulekh Chandra, Synthesis, characterization and biocidal properties of
626 platinum metal complexes derived from 2,6-diacetylpyridine (bisthiosemicarbazone),
627 Open Journal of Inorganic Chemistry, 2012, 2, 41-48.
- 628 [24]. Vojinović-Ješić Lj. S., Leovac V.M., Lalović M. M., Češljević V.I., Jovanović
629 Lj.S. Rodić M. V. and Divjaković V., Transition metal complexes with
630 thiosemicarbazide-based ligands. Part 58. Synthesis, spectral and structural
631 characterization of dioxovanadium(V) complexes with salicyl aldehyde
632 thiosemicarbazone, J. Serb. Chem. Soc., 2011, 76 (6), 865–877.
- 633 [25]. Baiu S.H., El-Ajaily M.M. and El-Barasi, Antibacterial Activity of Schiff Base
634 Chelates of Divalent Metal Ions, Asian Journal of Chemistry, (2009), 21(1), 5-10.
- 635 [26]. Elena Pahontu, Valeriu Fala, Aurelian Gulea, Donald Poirier, Victor Tapcov and
636 Tudor Rosu, Synthesis and Characterization of Some New Cu(II), Ni(II) and Zn(II)
637 Complexes with Salicylidene Thiosemicarbazones: Antibacterial, Antifungal and in
638 Vitro Antileukemia Activity, Molecules, 2013, 18, 8812-8836.
- 639 [27]. El-Bahnasawy R. M., Sharaf El-Deen L.M., El-Table A.S., Wahba M. A. and El-
640 Monsef. A., Electrical Conductivity Of Salicylaldehyde Thiosemicarbazone and its
641 Pd(II), Cu(II) and Ru(III) Complexes, Eur. Chem. Bull, 2014, 3(5), 441-446.

- 642 [28]. Md. Saddam Hossain, C.M. Zakaria, M.M.Haque, and Md. Kudrat-E-Zahan, Spectral
643 and thermal characterization with antimicrobial activity on Cr(III) and Sn(II)
644 Complexes containing N,O Donor novel schiff base ligand, International Journal of
645 Chemical Studies,2016, 4(6), 08-11.
- 646 [29]. A. Xavier, P. Gopu ,B. Akila,K. Suganya, Synthesis and Characterization of Schiff
647 Base from 3, 5-Di ChloroSalicylaldehyde with 4-Bromoaniline and 4-Aminobenzoic
648 Acid and Its 1st Row Transition Metal Complexes, International Journal Of
649 Innovative Research & Development, 2015, 4(8), 384-396 .
- 650 [30]. Manohar V. Lokhande and Mrityunjay R. Choudhary, Some Transitional Metal Ions
651 Complexes With 3-[(E)-(4-Fluorophenyl) Methylidene] Amino} Benzoic Acid And
652 Its Microbial Activity, International Journal of Pharmaceutical Sciences and
653 Research, IJPSR, 2014, 5(5), 1757-1766.
- 654 [31]. P. Gopu, Dr. A. Xavier,Synthesis and Characterization of 4-(3-bromo-5 -chloro-2-
655 hydroxybenzlidimino) Benzoic Acid and its Transition Metal Complexes,
656 International Journal of Science and Research (IJSR), 2015, 4,(8) 15-21.
- 657 [32]. Shanker K, Rohini R, Ravinder V and Reddy P M: Ru(II) complexes of N4 and N2O2
658 macrocyclic Schiff base ligands: Their antibacterial and antifungal studies, Spectro
659 chimica Acta A, 2009, 73, 1205-211.
- 660 [33]. Raju Ashokan, Saravanan Sathishkumar, Ekamparam Akila And Rangappan Rajavel,
661 Synthesis, Characterization and Biological Activity of Schiff Base Metal Complexes
662 Derived from 2, 4-Dihydroxyactophenone, Chemical Science Transactions , 2017,
663 6(2), 277-287 .
- 664 [34]. Miguel-Angel Munoz-Hernandes, Michal L. Mckee, Timothy S. Keizer, Burt C.
665 Yearwood and David Atwood, Six-coordinate aluminiumcations: characterization,
666 catalysis, and theory, 2002,3.
- 667 [35]. K. Nakamoto: Infrared Spectra of Inorganic and Coordination Compounds. John
668 Wiley & Sons, New York, 2nd Edition, 1970.
- 669 [36]. Shanker K B, Rohini M, Ravinder Reddy P and Ho M Y P: Synthesis of Tetraaza
670 Macrocyclic Pd(II) complexes; Antibacterial & Catalytic studies, J.of the Ind. Chem.
671 Soc. 2009, 86.
- 672 [37]. K.P. Satheesh, V. Suryanarayana Rao, Spectrophotometric Method For The
673 Determination Of Trace Amount Of Tungsten (Vi) In Alloy Samples Using 4-
674 Hydroxybenzaldehydethiosemicarbazon, Journal of Advanced Scientific Research,
675 2015, 6(2), 14-17.

- 676 [38]. S. Janarthanan, Y.C. Rajan, P.R. Umarani, D. Jayaraman, D. Premanand and S. Pandi,
677 Synthesis, growth, optical and thermal properties of a new organic crystal
678 semicarbazone of p-anisaldehyde, (SPAS), 2010, 3(8), 42-47.
- 679 [39]. Ruchi Agarwal, Mohd. Asif Khan and Shamim Ahmad, Schiff base complexes
680 derived from thiosemicarbazone, synthesis characterization and their biological
681 activity, Journal of Chemical and Pharmaceutical Research, 2013, 5(10), 240-245.
- 682 [40]. Sandra S. Konstantinovi, Blaga C. Radovanovi, Ivojin Caki And Vesna Vasi, Synthesis
683 and characterization of Co(II), Ni(II), Cu(II) and Zn(II) complexes with 3-
684 salicylidenehydrazono-2-indolinone, J.Serb.Chem.Soc., 2003, 68(8-9), 641-647.
- 685 [41]. N. K. Gondia, J. Priya, S. K. Sharma, Synthesis and physico-chemical
686 characterization of a Schiff base and its zinc complex, Res Chem Intermed, 2017,
687 43,1165-1178.
- 688 [42]. Lotf A. Saghatforoush, Ali Aminkhani, Sohrab Ershad, Ghasem Karimnezhad,
689 Shahriar Ghammamy and Roya Kabiri, Preparation of Zinc (II) and Cadmium (II)
690 Complexes of the Tetradentate Schiff Base Ligand 2-((E)-(2-(2(pyridine-2-yl)-
691 ethylthio)ethylimino)methyl)-4-bromophenol (PytBrsalH), Molecules 2008, 13, 804-
692 811.
- 693 [43]. Jian-Ning Liu, Bo-Wan Wu, Bing Zhang, Yongchun Liu, Synthesis and
694 Characterization of Metal Complexes of Cu(II), Ni(II), Zn(II), Co(II), Mn(II) and
695 Cd(II) with Tetradentate Schiff Bases, Turk J Chem., 2006,30, 41-48.
- 696 [44]. Shayma A. Shaker, Preparation and Spectral Properties of Mixed-Ligand Complexes
697 of VO(IV), Ni(II), Zn(II), Pd(II), Cd(II) and Pb(II) with Dimethylglyoxime and N-
698 Acetyl glycine, E-Journal of Chemistry, 2010, 7(S1), S580-S586.
- 699 [45]. Md. Kudrat-E-Zahan, M. S. Islam, and Md. Abul Bashar, Synthesis, Characteristics,
700 and Antimicrobial Activity of Some Complexes of Mn(II), Fe(III) Co(II), Ni(II),
701 Cu(II), and Sb(III) Containing Bidentate Schiff Base of SMDTC, Russian Journal of
702 General Chemistry, 2015,85(3),667-672.
- 703 [46]. Rehab K. Al-Shemary, Ahmed T. Numanand Eman Mutar Atiyah, Synthesis,
704 Characterization And Antimicrobial Evaluation Of Mixed Ligand Complexes Of
705 Manganese(Ii), Cobalt(Ii), Copper(Ii), Nickel(Ii) And Mercury(Ii) With 1,10-
706 Phenanthroline And A Bidentate Schiff Base, Eur. Chem. Bull., 2016, 5(8), 335-338.
- 707 [47]. Iniama, G.E., Olarele, O.S. and Johnson, A, Synthesis, spectral, characterization and
708 antimicrobial activity of manganese (II) and copper (II) complexes of

- 709 Salicylaldehydephenylhydrazone, International Journal of Chemistry and
710 Applications, 2015, 7(1), 15-23.
- 711 [48]. Neelofar, Nauman Ali, Shabir Ahmad, Naser M. Abdel-Salam, Riaz Ullah, Robila
712 Nawaz and Sohail Ahmad, Synthesis and evaluation of antioxidant and antimicrobial
713 activities of Schiff base tin (II) complexes, Tropical Journal of Pharmaceutical
714 Research ,2016,15(12), 2693-2700.
- 715 [49]. Har Lal Singh and J. B. Singh, Synthesis and Characterization of New Lead(II)and
716 Organotin(IV) Complexes of Schiff Bases Derived from Histidine and Methionine,
717 Hindawi Publishing Corporation, International Journal of Inorganic Chemistry,
718 2012,7pages.
- 719 [50]. Sunita Bhanuka and Har Lal Singh, Spectral, Dft And Antibacterial Studies Of Tin(Ii)
720 Complexes Of Schiff Bases Derived From Aromatic Aldehyde And Amino Acids,
721 Rasayan J. Chem., 2017, 10(2), 673-68.
- 722 [51]. Khalil Abid, Sinann Al-Bayati, Anaam Rasheed, Synthesis, Characterization,
723 Thermal study and Biological Evaluation of Transition Metal Complexes Supported
724 by ONNNO-Pentadentate Schiff Base Ligand, American Journal of Chemistry, 2016,
725 6(1), 1-7.
- 726 [52]. Allan J. R. and Veitch P. M., The preparation, characterization and thermal analysis
727 studies on complexes of cobalt(II) with 2-, 3-, 4-cyanopyridines, 1983, **J. Thermal**
728 **Anal.**, 27(1), 3-15.
- 729 [53]. Moamen S. Refat, I. M. El-Deen, M. S. El-Garib, and W. Abd El-Fattah,
730 Spectroscopic and Anticancer Studies on New Synthesized Copper(II) and
731 Manganese(II) Complexes with 1,2,4- Triazines Thiosemicarbazide1, Russian Journal
732 of General Chemistry, 2015, 85(3), 692–707.
- 733 [54]. Md. Saddam Hossain, Md. Ashraful Islam, C. M. Zakaria, M. M. Haque, Md. Abdul
734 Mannan, Md. Kudrat-E-Zahan, Synthesis, Spectral and Thermal Characterization with
735 Antimicrobial Studies on Mn(II), Fe(II), Co(II) and Sn(II) Complexes of Tridentate
736 N,O Coordinating Novel Schiff Base Ligand” J. Chem. Bio. Phy. Sci. Sec. A., 2016,6
737 (1),041-052.
- 738 [55]. M. R. Islam, J. A. Shampa, M. Kudrat-E-Zahan, M. M. Haque, Y. Reza, Investigation
739 on Spectroscopic, Thermal and Antimicrobial Activity of Newly Synthesized
740 Binuclear Cr(III) Metal Ion Complex , J. Sci. Res., 2016, 8 (2), 181-189.
- 741 [56]. Sayed M. Abdallah, M.A. Zayed, Gehad G. Mohamed, Synthesis and spectroscopic
742 characterization of new tetradentate Schiff base and its coordination compounds of

- 743 NOON donor atoms and their antibacterial and antifungal activity, *Arabian Journal of*
744 *Chemistry*, 2010, 3, 103–113.
- 745 [57]. Samir Alghool. Mononuclear complexes based on reduced Schiff base derived from L-
746 methionine, synthesis, characterization, thermal and in vitro antimicrobial studies, *J*
747 *Therm Anal Calorim*, 2015, 12, 1309–1319.
- 748 [58]. Achut S. Munde, Amarnath N. Jagdale, Sarika M. Jadhav And Trimbak K.
749 Chondhekar, Synthesis, characterization and thermal study of some transition metal
750 complexes of an asymmetrical tetradentate Schiff base ligand, *J. Serb. Chem. Soc.*,
751 2010, 75(3), 349–359.
- 752 [59]. A.S. Munde, V. A. Shelke, S. M. Jadhav, A. S. Kirdant, S. R. Vaidya, S. G.
753 Shankarwar, and T. K. Chondhekar, Synthesis, Characterization and Antimicrobial
754 Activities of some Transition Metal Complexes of Biologically Active Asymmetrical
755 Tetradentate Ligands, *Adv. Appl. Sci. Res.*, 2012, 3(1), 175-182.